Charles University
Faculty of Mathematics and Physics
Prague

MASTER'S THESIS

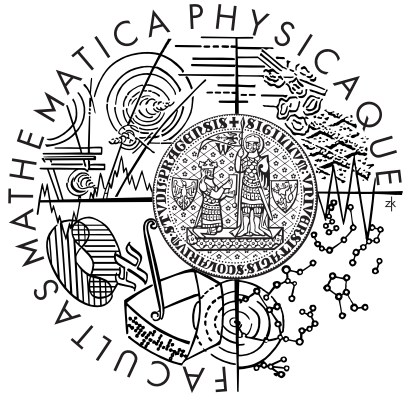

Vítězslav Štembera

The flow through visco-elastic tubes

Mathematical Institute of Charles University
Advisor: Prof. Ing. František Maršík DrSc.
Department: Department of mathematical modeling

Acknowledgments

I would like to thank my advisor Prof. Ing. František Maršík, DrSc. for all his support and help during the work. It was trully a pleasure to work with him. I thank to Doc. RNDr. Josef Málek, CSc. for his willingness to answer my questions concerning the theory of hyperbolic systems. I would also like to thank Jakub Otáhal for his help with my questions concerning the human body. I would also like to thank my friend Mgr. Štěpán Popelka for teaching me to use program Origin. I would like to thank everyone who showed interest and enthusiasm for my work.

I declare that I have set up this thesis by myself using the mentioned sources only. This work can be borrowed at will.

Prague, May 15, 2002

Vítězslav Štembera

To all positive people

"Everything, what really exists, is NOW."

Roshi Kosho Uchiyama

Contents

Notations

A	$[\mathrm{m}^2]$	cross-sectional area of the tube
A_0	$[\mathrm{m}^2]$	cross-sectional area of the rigid tube
A_0	$[\mathrm{m}^2]$	cross-sectional area of the flexible tube in undeformed state
$\widetilde{A} = \frac{A}{A_0}$		cross-sectional area of the tube in the non-dimensional form
$\check{A}$		cross-sectional area of the test rigid tube
D	[m]	diameter of the tube
D_0	[m]	diameter of the rigid tube
D_0	[m]	diameter of the flexible tube in undeformed state
E	$[\mathrm{N\,m^{-2}}]$	Young modulus
f	$[\mathrm{N\,kg^{-1}}]$	frictional force
f_u, f_d	$[\mathrm{N\,kg^{-1}}]$	frictional forces in rigid tubes
$\mathbf{F_1}, \mathbf{F_2}, \mathbf{F_W}$	[N]	surface forces acting on the element of the length L
$\mathbf{F_S}$	[N]	surface force acting on the element of the length L
F_V	$[\mathrm{N\,m^{-1}}]$	"length" density of the volume force
h	[m]	thickness of the tube wall
h	[m]	the spatial step in iterative process
I_L	$[\mathrm{kg\,m\,s^{-1}}]$	momentum of the element of the length L
J		Jacobian matrix
$J_C = \det J$		Jacobian
$\mathcal{J}(\Phi)$		flow of the extensive quantity Φ through the system boundary
$\mathbf{J}(\Phi)$		flow-density of the extensive quantity Φ
k	[m]	roughness of the tube
l	[m]	length of the flexible tube
l_u	[m]	length of the left rigid flexible tube
l_d	[m]	length of the right rigid flexible tube

m_L	[kg]	mass of the element of the length L
$\mathbf{n_1}, \mathbf{n_2}, \mathbf{n_W}$		outer normals corresponding to the element of the length L
N		number of nodes
p	[Pa]	pressure
$\widetilde{p} = \frac{p}{p_S}$		pressure in the non-dimensional form
p_S	[Pa]	pressure in reservoir
p_e	[Pa]	external pressure
p_I	[Pa]	pressure at the beginning of the left rigid part
p_u	[Pa]	pressure at the end of the left rigid part
p_d	[Pa]	pressure at the beginning of the right rigid part
p_E	[Pa]	pressure at the end of the right rigid part
$\mathcal{P}(\Phi)$		production of the extensive quantity Φ in the system
$Q = Av$	$[\mathrm{m^3 s^{-1}}]$	flux
Q_0	$[\mathrm{m^3 s^{-1}}]$	given fix flux
$\widetilde{Q} = \frac{Q}{Q_0}$		flux in the non-dimensional form
R	$[\mathrm{Pa^2 m^{-6}}]$	resistance of the restrictor
Re		Reynolds number
res		residuum
res_A		residuum of the system (5.33)
res_Q		residuum of the system (5.39), (5.40) and (5.43)
res_{MAX}		maximum residuum
res_{AMAX}		maximum residuum for the system (5.33)
res_{QMAX}		maximum residuum for the system (5.39) (5.40) and (5.43)
S	[m]	peripheral length of the tube
S_0	[m]	peripheral length of the rigid tube

S_0	[m]	peripheral length of the flexible tube in undeformed state
$\mathbf{v}, v$	$[\mathrm{m\,s^{-1}}]$	velocity
t	[s]	time
$\triangle t$	[s]	length of the time step in iterative process
T	$[\mathrm{N\,m^{-1}}]$	smoothness parameter
T	[°C]	temperature
V_L	$[\mathrm{m^3}]$	volume of the element of the length L
V_t		actual domain at the time t
V_{t_0}		referential domain at the time t_0
$\mathbf{w}$		solution vector
x_i		mesh points in A- and p-nodes
$\mathbf{x}, x$	[m]	actual coordinates
$\mathbf{X}$	[m]	referential coordinates
y	[m]	actual coordinate
y_i		mesh points in Q-nodes
λ		eigenvalue
λ_f		frictional coefficient
θ		parameter for the Euler and Crank-Nicholson method
κ	$[\mathrm{kg\,s^{-1}}]$	"length" density of momentum
μ	[Pa s]	dynamic viscosity
$\nu = \frac{\mu}{\rho}$	$[\mathrm{m^2 s^{-1}}]$	kinematic viscosity
$\sigma(\Phi)$		production-density of the extensive quantity Φ
χ	$[\mathrm{kg\,m^{-1}}]$	"length" density of mass
ω		relaxation parameter for the Newton method
ω		relaxation parameter for the SOR method
ω		relaxation parameter for the simple implicit method

$\Upsilon(\mathbf{X}, t)$	the mapping from the reference domain V_{t_0} to the actual domain V_t
$.^{\star}$	iterative value
$\acute{.}$	correction
$\hat{.}$	value from the previous time step
$\bar{.}$	value from the previous iterative step
$\text{div} = \sum_{i=1}^{3} \frac{\partial}{\partial x_i}$	divergence operator
$(SYST1)$	system of equations (3.72)-(3.82)
$(SYST2)$	system of equations (3.83), (3.84) and (3.75)-(3.82)

Chapter 1

Introduction

The disorder of the cardiovascular system invariably takes the leading rank in the medical statistics. Aproximately 190 people die daily as a consequence of heart and blood vessel diseases in the Czech Republic. Atherosclerosis (hardening of the arteries, see [8], [7]), is the chef cause of death in most of the western world. Therefore it makes sense to develop mathematical models simulating the blood flow through human vessels-arteries and veins. These models could help us to understand more the creation and continuance of vessel diseases. It is necessary to note that the task of modeling vessel diseases includes many different kinds of interactions. Apart of the purely mechanical behaviour like viscous fluid flow and elastic defomations it includes very complicated chemical and electric interactions. The simulation of vessel diseases would require a more complex model.
In this work we focus on the purely mechanical interactions involving viscous fluid and the visco-elastic tube. We derive a one-dimensional model considering that the fluid is incompressible and the tube has a thin wall. The process is considered to be isothermal. All assumptions of the model are summarized in Section 3.1.
Chapter 2 is devoted to the basic description of the human blood circulatory system. The problem formulation and the mathematical model are derived in Chapter 3, and some analytical properties of the system are discussed in Chapter 4. The model is studied numerically with four different numerical methods. These numerical methods are derived in Chapter 5 and Chapter 6 includes numerical results.

Chapter 2

Blood flow in the human body

In this thesis we deal with the model describing the flow through the visco-elastic tubes. The main area of applications is the blood flow through human vessels - arteries and veins. These models could help us to understand better vessels diseases like the atherosclerosis (hardening of the arteries, see [7], [8]), aneurysma of the abdominal aorta[1] (the crosswise enlargement of the abdominal aorta, see [6]) and others. We have to say that these diseases are very complex and apart from the purely mechanical behaviour they also include very complicated chemical and electric interactions. The complete description of these diseases requires a much more complex model than the one presented here. But this model could be the base for future extensions. This Chapter is devoted to the description of the human blood circulatory system (Section 2.1), the composition of the blood (Section 2.2) and the structure of the human vessels walls (Section 2.3).

2.1 Blood circulatory system

2.1.1 Blood circulatory system

There are two types of blood circulatory system, the systemic and pulmonary systems, which depend on a central pump, the heart, to push the blood around (see Figure 2.1).

1. **Systemic circulation**
   The systemic circulation transfers oxygenated blood from a central pump

[1] Aneurysma of the abdominal aorta was the cause of the death of Albert Einstein ([6]).

(the heart) to all of the body tissues (*systemic arterial system*) and returns deoxygenated blood with a high carbon dioxide content from the tissues to the central pump (*systemic venous system*).

2. **Pulmonary circulation**
   The pulmonary circulation transfers deoxygenated blood with a high carbon dioxide content from a central pump (the heart) to the lungs (*pulmonary arterial system*) and transfers reoxygenated blood from the lungs back to the central pump (*pulmonary venous system*).

The blood circulatory system consists of the heart and blood vessels.

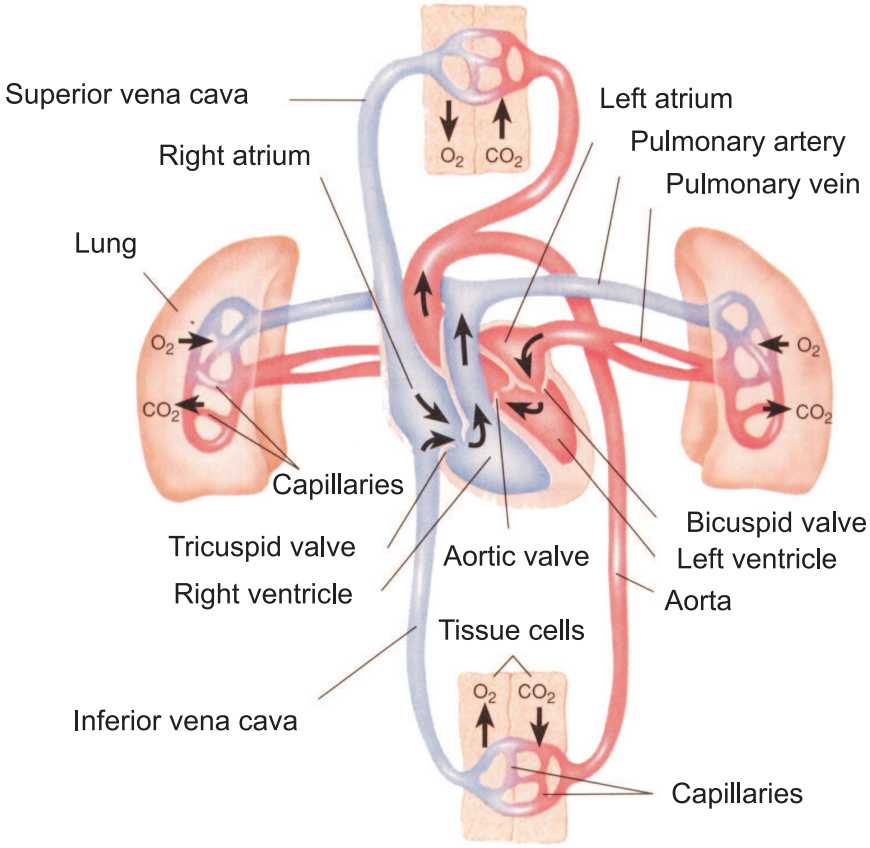

Figure 2.1: The diagram of the circulatory system

2.1.2 Heart

The *heart* is a muscular pump with four chambers.

1. Right atrium
   The *right atrium* receives deoxygenated blood from the systemic venous system.
2. Right ventricle
   The *right ventricle* pumps deoxygenated blood through the lungs (where the blood acquires oxygen) and then into the left atrium via pulmonary veins.
3. Left atrium
   The *left atrium* receives oxygenated blood from pulmonary veins.
4. Left ventricle
   The *left ventricle* pumps oxygenated blood throughout the body.

The heart of an adult pumps about 5 liters of blood per minute. It takes about 1 minute for blood to be circulated to the most distal extremity and back to the heart.

2.1.3 Blood vessels

Blood vessels that transport blood away from the heart are called *arteries* and those that take blood toward the heart are called *veins*.
Blood vessels form a tubular network that permits blood to flow from the heart to all the living cells of the body and then back to the heart. Arteries and veins are continuous with each other through smaller blood vessels.
Arteries branch extensively to form a "tree" of progressively smaller vessels. Those that are microscopic in diameter are called *arterioles*. Blood passes from the arterial to the venous system in *capillaries*. Then blood flows into microscopic-sized veins, called *venules*, which deliver blood into progresively larger veins that return the blood to the hearth.
Arteries and veins could be sub-divided into the following types

1. Arteries:
   - Arteries of large diameter (the so-called elastic type arteries) – the wall of these arteries contain a relatively high proportion of elastin[2] causing the characteristic yellow colouring of the wall. Their diameter is bigger than $10\,mm$.
   - Arteries of medium and small diameter (the so-called muscular type arteries) – their walls of considerable thickness are formed by

[2]Elastin is protein.

smooth muscles to a large proportion. Their diameter is approximately 400 μm to 10 mm.

- Arterioles – approximate diameter range 30-400 μm.
- Precapillaries – approximate diameter range 5-10 μm.

2. Veins:
   - Postcapillaries – approximate diameter range 5-10 μm.
   - Venules – approximate diameter range 10 μm-1 mm.
   - Veins of small and medium diameter – the diameter is approximately 1 mm-10 mm.
   - Veins of large diameter – their diameter is bigger than approximately 10 mm.

2.1.4 Cardiac cycle

The *cardiac cycle* refers to the repeating pattern of contraction and relaxation of the heart. The phase of contraction is called *systole* and the phase of relaxation is called *diastole*. When these terms are used without reference to specific chamber, they refer to contraction and relaxation of the ventricles. It should be noted, however, that the atria also contract and relax. There is an atrial systole and diastole. Atrial contraction occurs toward the end of diastole, when the ventricles are relaxed; when the ventricels contract during systole, atria are relaxed.
The heart thus has a two-step pumping action. The right and left atria contract almost simultaneously, followed by contraction of the right and left ventricles 0.1 to 0.2 second later.
At an average *cardiac rate* of 67.5 beats per minute, each cycle lasts 0.89 second; 0.54 second is spent in diastole, and systole takes 0.35 second (Figure 2.2). The diagram of the pressure in aorta during the cardiac cycle is shown on the Figure 2.3.

2.2 Composition of the blood

The average-sized adult has about 5 liter of blood, constituting about 8% of the total body weight. Blood leaving the heart is referred to as *arterial blood*, blood returning to the heart is referred to as *venous blood*.
Blood is composed of cellular portion, called *formed elements*, and a fluid portion, called *plasma*. The ratio between the volume of the formed elements

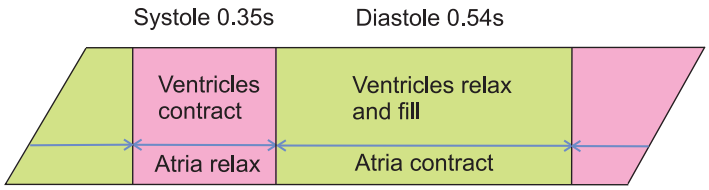

Figure 2.2: The cardiac cycle of a ventricular systole and diastole. The durations of systole and diastole given relate to a cardiac rate of 67.5 beats per minute.

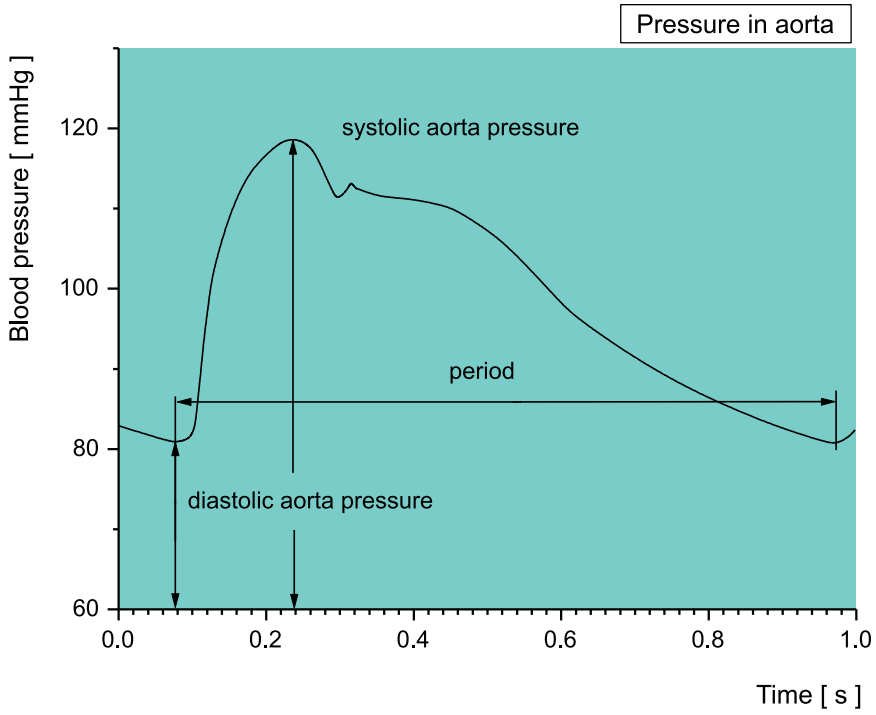

Figure 2.3: The diagram of the pressure in the aorta during the cardiac cycle. The period 0.89 s given to a cardiac rate of 67.5 beats per minute.

and the total blood volume is called *hematocrit*. The normal value is shown

in the following Table

	Hematocrit H
Female	42%
Male	45%

(2.1)

The hematocrit is the main factor which influences the viscosity of the blood (see Section 3.5). The hematocrit can be very high in adults living at very high altitudes (60%), 75% in polycythemia patients. On the other hand, the hematocrit can be as low as 20% to 25% in persons suffering from sickle-cell anemia or thalassemia ([4]). The value of the hematocrit could be also changed by drinking a lot of liquid, but after couple of hours the normal value is recovered.
In medium and large vessels (inner diameter $\geq 3\,mm$, see Section 2.1.3) the blood behaves like a Newtonian fluid. In smaller diameter blood behaves like non-Newtonian fluid. The major cause of such a behaviour is clustering of red blood cells and the minor one is an elastic deformation of the red blood cells as a consequence of the shear stress ([9]).

2.2.1 The formed elements of blood

Blood consists of the following formed elements:

1. **Erytrocytes** (**red blood cells**) :
   Red blood cells are flattened, biconcave discs, about $7\mu m$ in diameter and $2.2\mu m$ thick. They transport oxygen from the lungs to the peripheral tissues. A cubic millimetr of blood contains 5.1 to 5.8 million erytrocytes in males and 4.3 to 5.2 million erytocytes in females. Erytrocytes have a circulating life span of only about 120 days before they are destroyed by phagocytic cells in liver, spleen, and bone marrow.
2. **Leukocytes** (**white blood cells**) :
   Leukocytes are oval cells, about $5 - 17\mu m$ in diameter. Leukocytes can move in an amoeboid fashion (erytrocytes are not able to move independently). Because of their amoeboid ability, leukocytes can squeeze through pores in capillary walls and move to a site of infection, whereas erytrocytes usually remain confined within blood vessels. A cubic millimetr of blood contains 5000 to 9000 leukocytes. The lack of leukocytes is the cause of the leukaemia. There are several types of leukocytes : *neutrophils*, *eosinophils*, *basophils*, *lymphocytes* and *monocytes*.

3. **Platelets**
   Platelets, or *trombocytes*, are the smallest of the formed elements. The platelets play an important role in blood clotting. Platelets, like leukocytes, are capable of amoeboid movement. The platelets count per cubic millimetr of blood is 250.000 to 450.000. Platelets survive about 5 to 9 days before being destroyed by the spleen and liver.

2.3 Blood vessel walls

The systemic circulation is an extensive high pressure system and the structure of its proximal vessels reflects the high pressures to which they are subjected. Furthermore they are modified to smooth the flow of blood, since blood is impelled through them only during systole, and it is important to maintain an adequate pressure and flow during the diastolic intervals.
The structural modifications to handle the high systolic pressure and to maintain a respectable diastolic pressure are most refined in large *elastic arteries*, which receive the output of the left ventricle (i.e. the aorta and its large branches). Distal to these large elastic arteries, the artery walls gradually become more muscular (i.e. *muscular arteries*). (The classification of the blood vessels by size is in Section 2.1.3.)

2.3.1 General structure

The walls of large and medium sized arteries have three identifiable layers. In veins these three layers are less clearly defined, and in small blood vessels (i.e. arterioles, capillaries and venules, see Section 2.1.3) they are so narrow that they are virtually indistinguishable.
The layers are the intima, media and adventitia.

- Intima
  The *intima* is the thin inner layer of a blood vessel wall. It is lined internally by flat *endothelian cells*, which normally provide a smooth, friction-free internal surface, permitting the free flow of blood. In certain vessels the endothelial cells may be more cuboidal.
  The endothelial cells lie on a basement membrane, beneath which is a usually thin layer of collagen[3] fibres. In large vessels, the elastic fibres may aggregate at the lower border of the intima to form a distinct

[3]Collagen is protein.

internal elastic lamina, which is well-defined in muscular arteries, but indistinct in veins and elastic arteries.

- Media
  The *media* is the middle layer in a blood vessel wall and is particularly prominent in arteries, being indistinct in veins and virtually non-existent in very small vessels (e.g. capillaries). The composition of the media accounts for the main difference between elastic and muscular arteries (see below).
- Adventitia
  The *adventitia* is the outer layer of blood vessels, and is composed largely of collagen, but smooth muscle cells may be present, particularly in veins. In arteries it is demarcated from the media by a condensation of elastic fibres that forms a variably distinct *externa elastic lamina*. The adventitia is the most prominent layer in the walls of the veins.

2.3.2 Elastic arteries

Elastic arteries are the largest arteries and receive the main output of the left ventricle, thus they need to withstand the high systolic pressure of $120 - 160\,mm\,Hg$ and to maintain an adequate pressure during diastole.

- Media
  Elastic arteries have a thick, highly developed media in which elastic fibres are the main component, and are gathered together in sheets arranged in concentric layers throughout the thickness of the media. In the largest artery, the aorta, there are often 50 or more layers (see Figure 2.6).
  The elastic fibres are arranged so that they run circumferentially rather than longitudinnaly in order to counteract the tendency for the vessel to over-distent during systole. Return of the elastic fibres from their stretched to unstreched state during diastole maintains a diastolic pressure within the aorta and large arteries of about $60 - 90\,mm\,Hg$. Interposed between the elastic layer are smooth muscle cells and some collagen.

2.3.3 Muscular arteries

The large elastic arteries gradually merge into muscular arteries by losing most of their medial elastic sheets, usually leaving only two layers, an internal

elastic lamina and an external elastic lamina, at the junction of the media with the intima and adventitia, respectively.

- Media
  In a muscular artery the media is composed almost entirely of smooth muscle. these arteries are therefore highly contractile, their degree of contraction or relaxation being controlled by the autonomic nervous system. A few fine elastic fibres are scattered amongst the smooth muscle cells, but are not organized into sheets, and are a direct continuation of the distal end of the elastic arteries.
  Muscular arteries vary in size from about $10\,mm$ in diameter shortly after their origin from the elastic arteries, to about $400\,\mu m$ in diameter. In the larger arteries there may be 30 or more layers of smooth muscle cells, whereas in the smallest peripheral arteries, there are only 2 or 3 layers. The smooth muscle cells are usually arranged circumferentially at right angles to the long axis of the vessel.
  The internal elastic lamina is commonly a distinct prominent layer, but the external elastic lamina is less well defined, and is often discontinuous.

The following Table presents the inner diameter and the wall thickness of some arteries for the healthy adult (taken from [4]):

	inner diameter [mm]	wall thickness [mm]
Thoracic aorta	20.0	1.2
Abdominal aorta	11.4	0.8
Brachial artery	5.6	0.55
Femoral artery	3.8	0.5

(2.2)

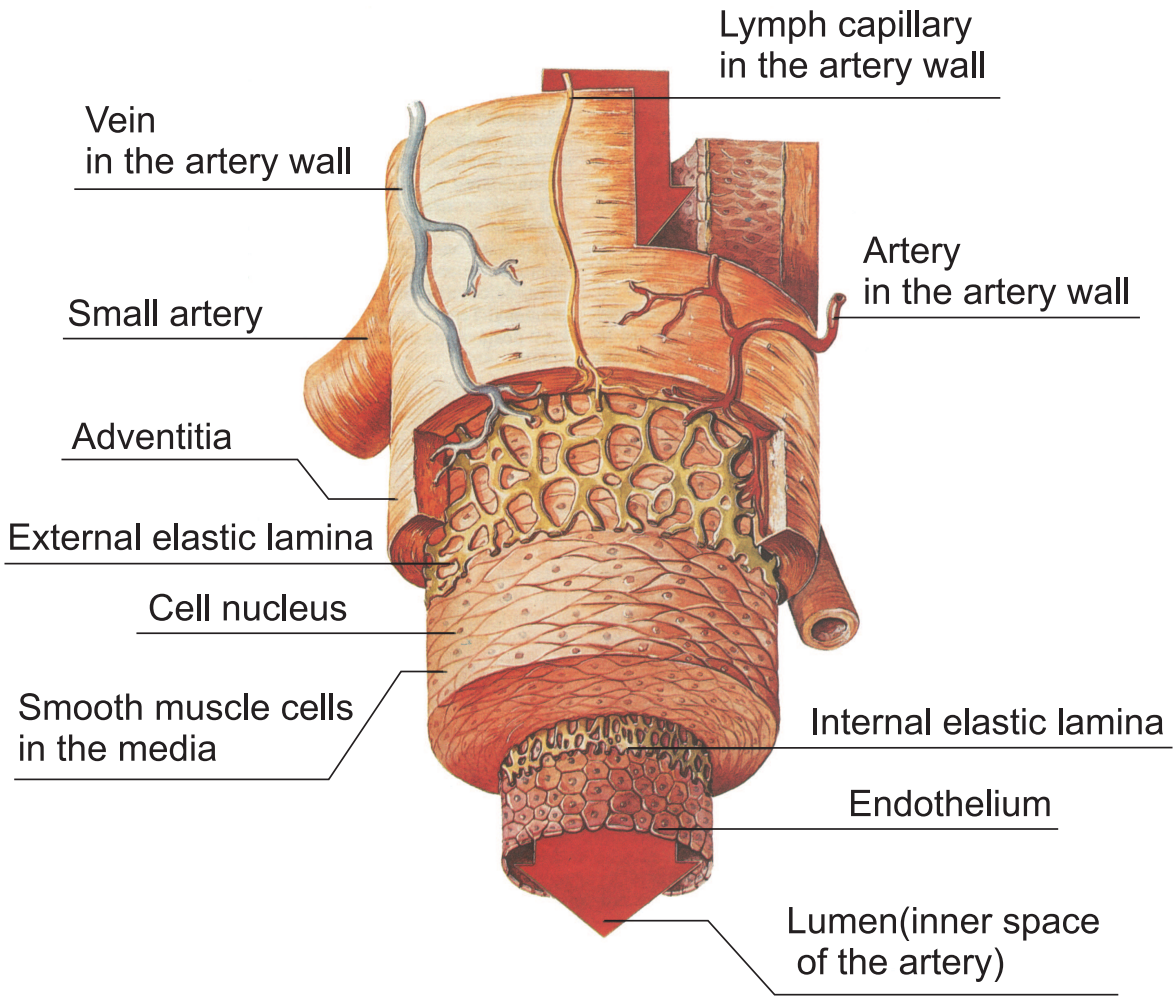

Figure 2.4: Muscular artery.

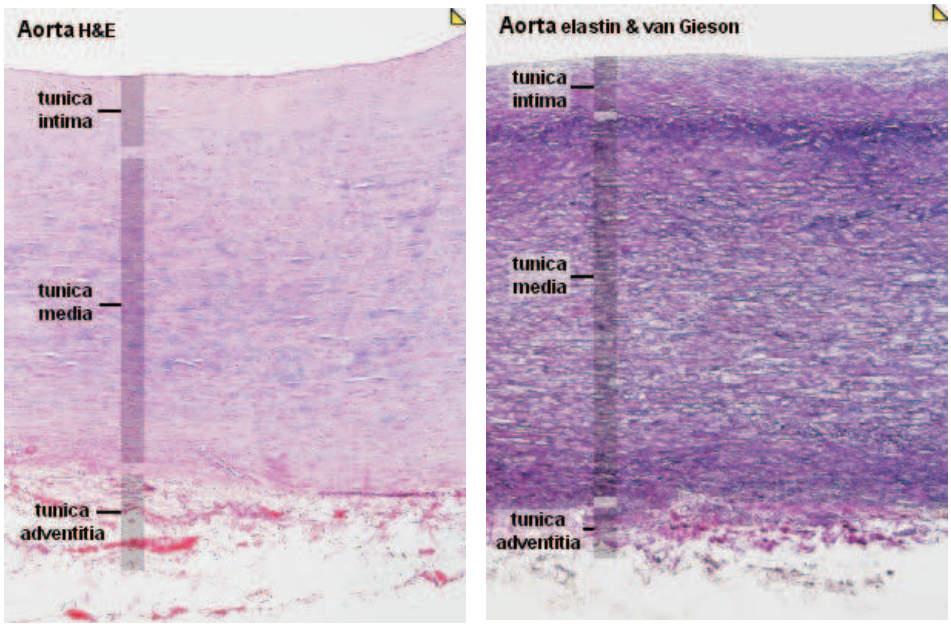

Figure 2.5: The structure of the aorta wall. (Figure on the right side is colored to the amount of elastin. It is possible to recognize interna and externa elastic lamina.

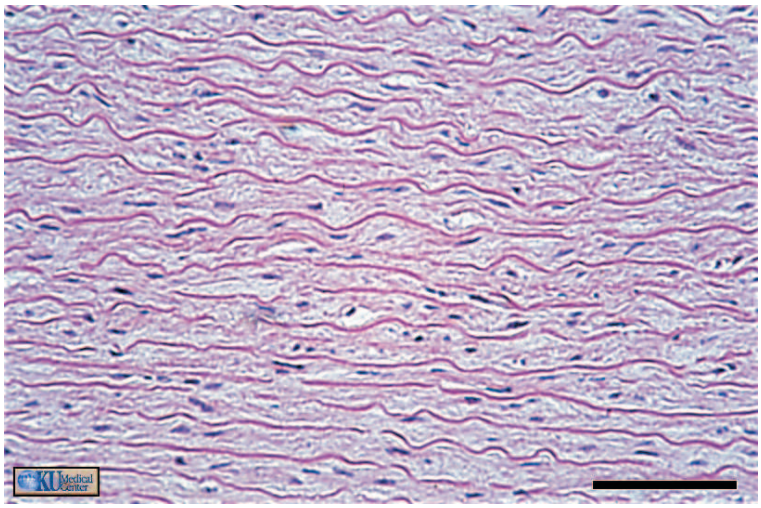

Figure 2.6: Elastic fibres in aorta media (Bar = 100 μm).

Chapter 3

Problem formulation

The aim of this study is to show the relationship between flow and artery wall conditions at physiological and pathological states.
In this Chapter we derive two mathematical models for the flow through elastic and visco-elastic tubes. The main area of applications will be modeling the blood flow through middle and large arteries (see previous Chapter for the definition). We make the following assumptions:

1. We use one dimensional approximation.
2. The fluid is considered as incompressible and Newtonian.
3. The tube is considered to be thin-walled, with constant thickness h. The material of the tube is homogennous with elastic or visco-elastic properties (according to model, see Section 3.6, 3.7).
4. The process is isothermal. (T = const.)
5. Only mechanical properties are modeled - no chemical interactions are included.

Figure 3.1 shows the tube system treated in this thesis. The flexible part is surrounded by two rigid channels. The flexible part has the length l, the left rigid part has the length l_u and the right part has the length l_d . The cross-sectional area of the tube is denoted by $A(x,t)$, the cross-sectional area of rigid parts is denoted by A_0. The thickness of the flexible tube is h, independent from x. The volume element dV between $x_1, x_2 \in \langle 0, l \rangle$ is given by

$$dV = \int_{x_1}^{x_2} A(x,t)dx \tag{3.1}$$

The fluid flows from the reservoir with constant pressure p_S. The pressure at the beginning and at the end of the left rigid part is denoted by p_I, and p_u respectively and analogously the pressure at the beginning and at the end of the right rigid tube is denoted by p_d and p_E respectively. The right rigid part ends with the restrictor. The flexible part of the tube is in the box with the pressure p_e, see Figure 3.1. The pressure behind the restrictor is assumed to be 0.

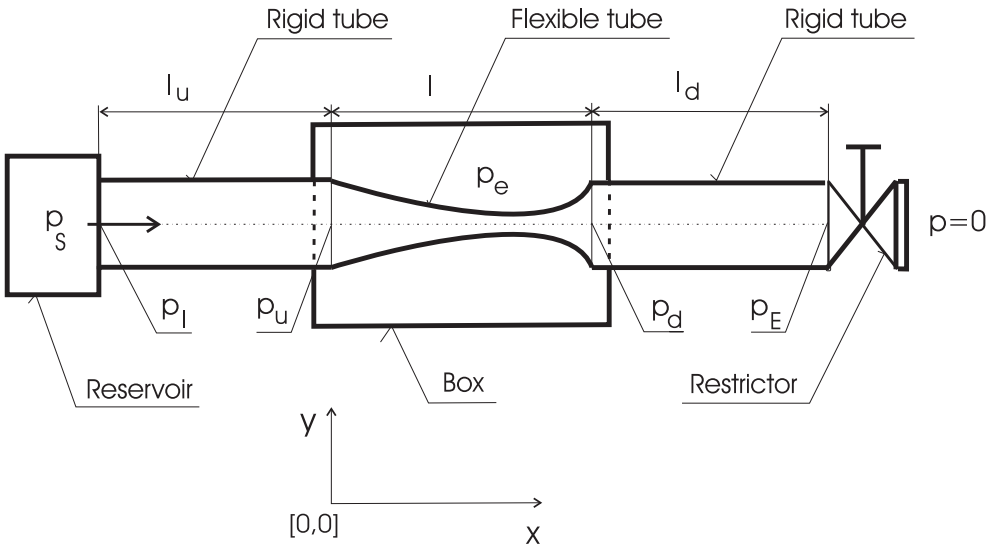

Figure 3.1: Schematic diagram of modeled tube system.

In Section 3.2 we look at the derivation of the general form of balance laws, in 3.3 we derive the balance of mass and momentum. The constitutive laws are introduced in Section 3.4. In Section 3.5 the density and viscosity of the blood are discussed. The derived models are summarized in Sections 3.6 and 3.7.

3.1 Continuum theory

We investigate the motion of fluid occupying a domain $V_t \subset \mathbf{R}^3$ at instant $t \in (T_1, T_2)$. We take an arbitrary instant $t_0 \in (T_1, T_2)$ and we assume that the referential domain $V_{t_0} \subset \mathbf{R}^3$ is bounded, with the Lipschitz-continuous boundary. The motion of fluid is described by the mapping

$$\Upsilon : V_{t_0} \subset \mathbf{R}^3 \times (T_1, T_2) \to V_t \subset \mathbf{R}^3, \quad \mathbf{x} = \Upsilon(\mathbf{X}, t), \quad t \in (T_1, T_2), \quad (3.2)$$

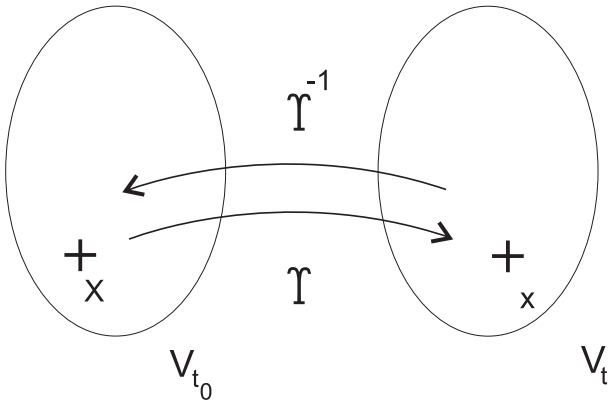

Figure 3.2: The mapping Υ and Υ^{-1} between the referential domain V_{t_0} and the actual domain V_t.

where $\mathbf{X}$ denotes the position of an arbitrary material point in V_{t_0} and the $\mathbf{x}$ denotes the position of this point in V_t at the time t. We suppose that the mapping Υ is injective and has the continuous partial derivatives with respect to $\mathbf{X}$ and t. Let t be an arbitrary fixed time instant from the interval (T_1, T_2). By $J_C = J_C(\mathbf{X}, t)$ we denote the Jacobian of the mapping $\Upsilon(\mathbf{X}, t)$

$$J_C(\mathbf{X}, t)(\mathbf{X}) = \det\left(\frac{\partial \Upsilon}{\partial \mathbf{X}}\right). \tag{3.3}$$

Under above mentioned assumptions the inverse mapping $\Upsilon^{-1}(\mathbf{x}, t)$ exists and the following equalities hold

$$\begin{aligned} \frac{\partial \Upsilon}{\partial \mathbf{X}} \frac{\partial \Upsilon^{-1}}{\partial \mathbf{x}} &= I(\mathbf{x}), \\ \frac{\partial \Upsilon^{-1}}{\partial \mathbf{x}} \frac{\partial \Upsilon}{\partial \mathbf{X}} &= I(\mathbf{X}), \end{aligned} \tag{3.4}$$

where $I(\mathbf{x})$, $I(\mathbf{X})$ are identities on V_t and V_{t_0} respectively. Above mentioned assumptions imply that one material point could not be at two different positions at the same time and two different points could not be at the same position at the same time.
The velocity is defined as the time derivative of the position

$$\mathbf{v}(\mathbf{X}, t) = \frac{\partial}{\partial t} \Upsilon(\mathbf{X}, t). \tag{3.5}$$

In continuum mechanics actual coordinates $\mathbf{x}$ instead of reference coordinates $\mathbf{X}$ are often used. Using the inverse mapping of $\Upsilon^{-1}(\mathbf{x}, t)$ the last equality

could be rewritten

$$\mathbf{v}(\mathbf{x},t) = \frac{\partial}{\partial t}\Upsilon(\Upsilon^{-1}(\mathbf{x},t),t). \tag{3.6}$$

We can use the same idea for an arbitrary quantity to make the transformation from reference coordinates to actual coordinates and vice versa.

3.2 General balance laws

Physical quantities are divided into two groups - *extensive* and *intensive* ones. Quantity $\Phi(t)$ is called extensive if its magnitude is proportional to the mass of the system (for example momentum, energy) or intensive if its magnitude is not proportional to the mass of the system (for example pressure, temperature).
The density $\varphi(\mathbf{x},t)$ of every extensive quantity $\Phi(t)$ is defined as

$$\varphi(\mathbf{x},t) = \lim_{\triangle V \to 0} \frac{\triangle \Phi(t)}{\triangle V}. \tag{3.7}$$

$\varphi(\mathbf{x},t)$ is the intensive quantity. The magnitude of $\Phi(t)$ in volume V_t is then given by

$$\Phi(t) = \int_{V_t} \varphi(\mathbf{x},t) dV. \tag{3.8}$$

Let us now deal with an arbitrary extensive scalar quantity $\Phi(t)$, sufficiently smooth (a vector or tensor quantity could be proceed analogously). Empiricaly we know that the change of the magnitude of the quantity $\Phi(t)$ in the system in a time has just two reasons:

1. the inflow / outflow of the quantity $\Phi(t)$ through the system boundary,
2. the source / sink of the quantity $\Phi(t)$ inside the system.

This can be formulated as

$$\frac{d}{dt}\Phi(t) = \mathcal{J}(\Phi) + \mathcal{P}(\Phi), \tag{3.9}$$

where $\mathcal{J}(\Phi)$ is the *flow* of the quantity $\Phi(t)$ through the boundary and $\mathcal{P}(\Phi)$ the *production* of the quantity $\Phi(t)$ inside the system. The flow and

production are

$$\mathcal{J}(\Phi) = \int_{\partial V_t} \mathbf{J}(\Phi) dS, \tag{3.10}$$

$$\mathcal{P}(\Phi) = \int_{V_t} \sigma(\Phi) dV, \tag{3.11}$$

where the vector variable $\mathbf{J}(\Phi)$ is the *flow-density* and $\sigma(\Phi)$ is the *production-density* of the quantity $\Phi(t)$. The substitution (3.8), (3.10) and (3.11) into (3.9) gives

$$\frac{d}{dt} \int_{V_t} \varphi(\mathbf{x}, t) dV = \int_{\partial V_t} \mathbf{J}(\Phi) dS + \int_{V_t} \sigma(\Phi) dV. \tag{3.12}$$

To derive the term on the left hand side of (3.12) we use the transport theorem (see Appendix 7.1) which respects that not only integrand but also the domain V_t are time dependent.
Using the transport theorem, we rewrite (3.12) as

$$\int_{V_t} \left[\frac{\partial}{\partial t} \varphi(\mathbf{x}, t) + \operatorname{div}(\varphi(\mathbf{x}, t)\mathbf{v}(\mathbf{x}, t)) \right] dV = \int_{\partial V_t} \mathbf{J}(\Phi) dS + \int_{V_t} \sigma(\Phi) dV. \tag{3.13}$$

It is possible to rewrite the first term on the right hand side using the Green theorem

$$\int_{V_t} \left[\frac{\partial}{\partial t} \varphi(\mathbf{x}, t) + \operatorname{div}(\varphi(\mathbf{x}, t)\mathbf{v}(\mathbf{x}, t)) \right] dV = \int_{V_t} \frac{\partial \mathbf{J}^k}{\partial \mathbf{x}^k} dV + \int_{V_t} \sigma(\Phi) dV. \tag{3.14}$$

Since the integral form of balance law (3.14) is valid for an arbitrary sub-domain $\tilde{V}_t \subset V_t$, the equation (3.14) also holds for integrands (the so-called divergence form)

$$\frac{\partial}{\partial t} \varphi(\mathbf{x}, t) + \operatorname{div}(\varphi(\mathbf{x}, t)\mathbf{v}(\mathbf{x}, t)) - \frac{\partial \mathbf{J}^k}{\partial \mathbf{x}^k} - \sigma(\Phi) = 0. \tag{3.15}$$

Remark 1

For 1D aproximation i.e. if we consider only one space variable, for an extensive quantity $\Phi(t)$ the density of the quantity $\Phi(t)$ is defined by

$$\varphi(x, t) = \lim_{\triangle x \to 0} \frac{\triangle \Phi(t)}{\triangle x}. \tag{3.16}$$

We will call it the "length" density.

3.3 Balance laws for quasionedimensional flexible tube

Considering the tube element of the length L and volume V_L, see Figure 3.3, we can formulate the balance laws as follows.

3.3.1 Balance of mass

According to the previous Chapter we look for the "length" density of the mass quantity i.e. we look for quantity $\chi(x,t)$ such that

$$m_L(t) = \int_L \chi(x,t)dx; \quad L \subset \langle 0, l\rangle, \tag{3.17}$$

where m_L is a mass of the volume of the length L (see Figure 3.3).
It is

$$\chi(x,t) = A(x,t)\rho, \tag{3.18}$$

because

$$\int_L A(x,t)\rho dx = \rho \int_L A(x,t)dx \underbrace{=}_{using(3.1)} \rho V_L = m_L. \tag{3.19}$$

We note that $\rho = \text{const.}$. Balance of mass is similar to (3.12) written as

$$\frac{d}{dt}\int_L \chi(x,t)dx = 0, \tag{3.20}$$

since both terms on the right hand side of (3.12) are zero. Using the equation (3.15) and the fact that last two terms on the left hand side of (3.15) are zero we can write directly

$$\rho\left[\frac{\partial}{\partial t}A(x,t) + \frac{\partial}{\partial x}(A(x,t)v(x,t))\right] = 0, \tag{3.21}$$

or

$$\frac{\partial}{\partial t}A(x,t) + \frac{\partial}{\partial x}(A(x,t)v(x,t)) = 0. \tag{3.22}$$

3.3.2 Balance of momentum

As mentioned in Chapter (3.2) we look for the "length" density of the momentum quantity in one dimension. For the element of the length L and volume V_L we look for $\kappa(x,t)$ such that

$$I_L(t) = \int_L \kappa(x,t)dx, \tag{3.23}$$

where $I_L(t)$ is the momentum of the element.
It is

$$\kappa(x,t) = \rho A(x,t)v(x,t), \tag{3.24}$$

because of

$$\int_L \rho A(x,t)v(x,t)dx \underbrace{=}_{using(3.1)} \int_{V_L} \rho v(x,t)dV = \int_{m_L} v(x,t)dm = I_L, \tag{3.25}$$

where $dm = \rho dV$. The last equation (3.25) is just the definition of the momentum I_L of the element of the length L. Using the formula (3.12) from the Section (3.2), where $\sigma(I)$ represents volume force (we denote it F_V) acting on the element, and denoting the first term on the right side by F_S^x we obtain the balance law in the form

$$\frac{d}{dt}\int_L \kappa(x,t)dx = F_S^x + \int_L F_V(x,t)dx. \tag{3.26}$$

The F_S^x is the x-component of the total surface force $\mathbf{F_S}$ acting on the element (see Figure 3.3). This formula represents nothing else then the second Newton law applied to the element of the length L in the x direction : the change of momentum is given by sum of acting forces.
Now we turn our attention to the left side of the equation (3.26). Using the transport theorem (see Appendix 7.1), (3.24) and the continuity equation (3.22) we have

$$\begin{aligned}
&\frac{d}{dt}\int_L \rho A(x,t)v(x,t)dx = \qquad (3.27)\\
&= \rho\int_L \left[\frac{\partial}{\partial t}\left(A(x,t)v(x,t)\right) + \frac{\partial}{\partial x}\left(A(x,t)v^2(x,t)\right)\right]dx =\\
&= \rho\int_L \left[\left(\frac{\partial}{\partial t}A(x,t) + \frac{\partial}{\partial x}(A(x,t)v(x,t))\right)v(x,t) + \right.\\
&\left. + \left(\frac{\partial}{\partial t}v(x,t) + v(x,t)\frac{\partial}{\partial x}v(x,t)\right)A(x,t)\right]dx =\\
&\underbrace{=}_{Using(3.22)} \rho\int_L \left[A(x,t)\left(\frac{\partial}{\partial t}v(x,t) + v(x,t)\frac{\partial}{\partial x}v(x,t)\right)\right]dx.
\end{aligned}$$

We express now the force F_S^x on the right hand side of equation (3.26). We neglect viscous losses in the fluid for a while and we deal only with pressure forces. We handle viscous losses like volume forces, see the next Section.

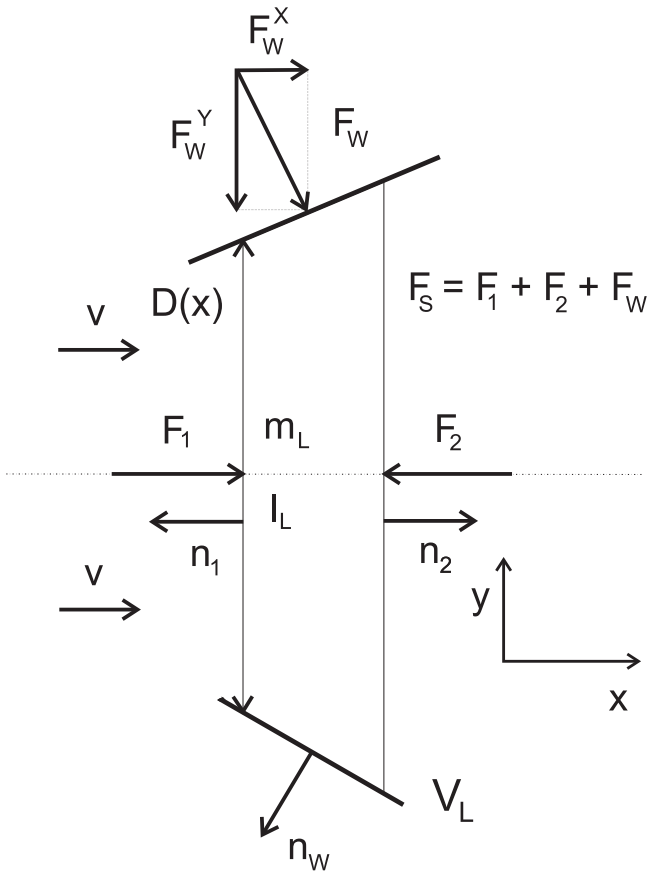

Figure 3.3: The forces acting on the tube element of the length L and the volume V_L, $\mathbf{n_1}$,$\mathbf{n_2}$ and $\mathbf{n_W}$ are outer normals of the surface ∂V_L and $\mathbf{F_1}$,$\mathbf{F_2}$ and $\mathbf{F_W}$ are the surface forces.

The element of the length L and volume V_L is affected by three surface forces $\mathbf{F_1}$, $\mathbf{F_2}$ and $\mathbf{F_W}$. $\mathbf{F_1}$ and $\mathbf{F_2}$ are pressure forces of surrounding fluid. Force $\mathbf{F_W}$ is the reaction to the pressure force of the fluid acting to the wall, see Figure 3.3. Using Taylor series expansion we can write for the x-components

$$
\begin{aligned}
&F_1^x(x) = p(x)A(x), \qquad (3.28)\\
&F_2^x(x) = -p(x+h)A(x+h) =\\
&= -\left(p(x) + \frac{\partial p(x)}{\partial x}h + O(h^2)\right)\left(A(x) + \frac{\partial A(x)}{\partial x}h + O(h^2)\right) =
\end{aligned}
$$

$$= -p(x)A(x) - A(x)\frac{\partial p(x)}{\partial x}h - p(x)\frac{\partial A(x)}{\partial x}h + O(h^2) \tag{3.29}$$

The surface force $\mathbf{F_W} = (F_W^x, F_W^y)$ is decomposed into x and y directions (see Figure 3.3). We can write for the x-component F_W^x

$$F_W^x = \int_x^{x+h} p(s)\frac{\partial A(s)}{\partial x}ds = \frac{\partial A(x)}{\partial x}p(x)h + O(h^2). \tag{3.30}$$

The force F_W^y is compensated by the lower side of the tube and is not taken into account for that moment. The total acting force in x direction is

$$F_S^x(x) = F_1^x(x) + F_2^x(x) + F_W^x(x) = -A(x)\frac{\partial p(x)}{\partial x}h + O(h^2). \tag{3.31}$$

Using (3.16) we determine the "length" density of the x-component F_S^x as follows

$$F_S^x = -\int_L A(x)\frac{\partial p(x)}{\partial x}dx. \tag{3.32}$$

Putting this formula into (3.26), using (3.27) we conclude that

$$\rho\int_L \left[A(x,t)\left(\frac{\partial}{\partial t}v(x,t) + v(x,t)\frac{\partial}{\partial x}v(x,t) + \frac{1}{\rho}\frac{\partial}{\partial x}p(x,t)\right)\right]dx = \int_L F_V(x,t)dx. \tag{3.33}$$

Coming to the divergence form and dividing by the ρ and $A(x,t)$ we finally obtain

$$\frac{\partial v(x,t)}{\partial t} + v(x,t)\frac{\partial v(x,t)}{\partial x} + \frac{1}{\rho}\frac{\partial p(x,t)}{\partial x} = \frac{F_V(x,t)}{\rho A(x,t)}. \tag{3.34}$$

We simply denote

$$f(x,t) = \frac{F_V(x,t)}{\rho A(x,t)}, \tag{3.35}$$

where f is the frictional force acting on the unit mass. We have in mind that f has the unit $[Nkg^{-1}]$, and F_V has unit $[Nm^{-1}]$.

3.3.3 Balance of momentum in rigid parts

In the previous two Subsections the properties of the fluid and the tube depend on coordinate x, the so-called distributed parameters. For the rigid

part the partial differential equations are transformed to ordinary differential equations.
The rigid parts and corresponding quantities are illustrated on Figure 3.4. The velocity is assumed to be constant along the tube. Using the second Newton law we can write

$$\frac{dv_u}{dt} = \frac{p_I - p_u}{\rho l_u} + f_u, \tag{3.36}$$

$$\frac{dv_d}{dt} = \frac{p_d - p_E}{\rho l_d} + f_d, \tag{3.37}$$

where the first term on the right side represents the force acting on one kilogram of the fluid and the second term represents the frictional losses. Terms f_u, f_d are given by

$$f_u = -\frac{\lambda_f}{8}\frac{S_0}{A_0} v_u |v_u| \left[\frac{N}{kg}\right], \tag{3.38}$$

$$f_d = -\frac{\lambda_f}{8}\frac{S_0}{A_0} v_d |v_d| \left[\frac{N}{kg}\right]. \tag{3.39}$$

There is further comment on this formula in Section 3.4.1, λ_f is given by (3.51).
The pressure p_I at the inlet is given by the Bernoulli law

$$p_S = p_I + \frac{1}{2}\rho v_u^2. \tag{3.40}$$

The pressure outside of the tube is zero. If the tube ended without the restrictor, we would put directly $p_E = 0$. The frictional losses of the restrictor could be related to pressure losses using the following empirical formula ([10])

$$p_E - 0 = R A_0^2 v_d |v_d|, \tag{3.41}$$

where $R[Pas^2m^{-6}]$ is the resistance of the restrictor.

3.4 Constitutive relations

3.4.1 Friction in the tube

We provide that the right hand side of equation (3.34) express frictional losses. The Reynolds number Re is a measure of flow quality. For the flow in tubes is defined as

$$\mathrm{Re} = \frac{|v|D}{\nu}, \tag{3.42}$$

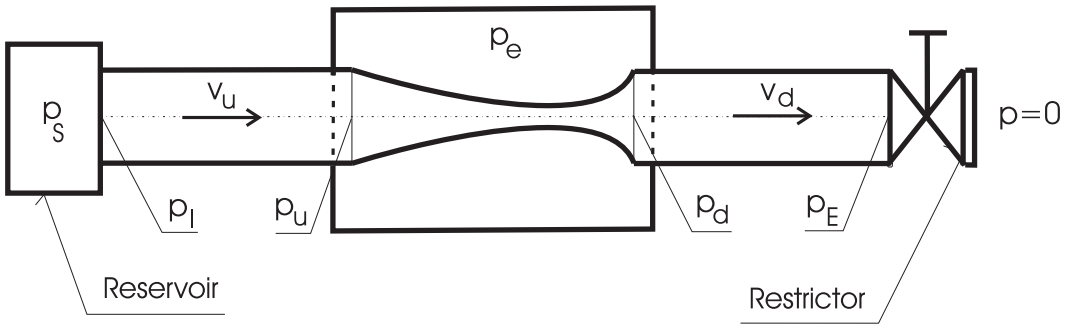

Figure 3.4: The velocity and pressure in rigid channels in modeled tube system.

where $\nu\,[m^2 s^{-1}]$ is the kinematic viscosity of the fluid, D the diameter of the tube and v the average velocity. For the laminar flow (approx. Re ≤ 2300) we can use the Poisseuille law (see [11]) which determines the relation between pressure drop $\triangle p$ on the tube of the length l and the cross-sectional area A and cross-sectional average velocity v in the following form

$$v = \frac{\triangle pA}{8\pi\mu l}, \tag{3.43}$$

where μ is dynamic viscosity given by the relation

$$\mu = \rho\nu \quad [Pa\,s]\,. \tag{3.44}$$

Using (3.35) and (3.43) we have

$$f = -\frac{1}{\rho A}\frac{\triangle pA}{l} = -\frac{8\pi\mu v}{A\rho} \quad \left[\frac{N}{kg}\right]. \tag{3.45}$$

The sign $-$ means that the frictional force acts always in the opposite direction than the fluid moves. We rewrite (3.45) to the equivalent form

$$f = -\frac{8}{\mathrm{Re}}\frac{S}{A}v|v|^1 \tag{3.46}$$

where $S = \pi D$ is peripheral length of tube tube.
For the Re approximately between 2300 and 4000 the flow comes into the transient regime and no formula exists. For the Re ≥ 4000 the turbulent regime occurs and the frictional losses increase (one order approximately). In this case dozens of empirical formulae exist to determine frictional losses. All of them have the form

$$f = -\frac{\lambda_f}{8}\frac{S}{A}v|v| \left[\frac{N}{kg}\right], \tag{3.47}$$

where λ_f is given by the empirical formula. The following is the Colebrook-White formula ([12])

$$\frac{1}{\sqrt{\lambda_f}} = 2\log\left[\frac{\sqrt{\lambda_f}\mathrm{Re}}{1+0.1\frac{k}{D_0}\sqrt{\lambda_f}\mathrm{Re}}\right] - 0.8, \tag{3.48}$$

where k is the roughness of the inner surface of the tube. Other empirical formulae are found in ([10]). We assume that $k = 0$, moreover, we replace this formula, where λ_f is given implicitly by the following explicit formula

$$\lambda_f = 1.02(\log \mathrm{Re})^{-2.5}. \tag{3.49}$$

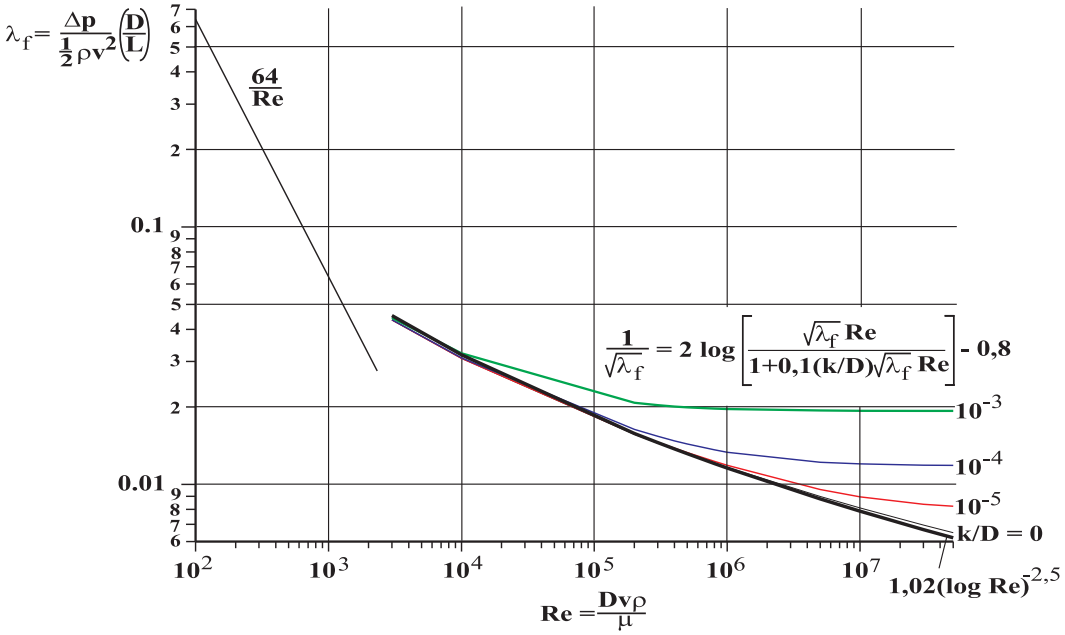

Figure 3.5: The dependence of the frictional coefficient λ_f on the Reynolds number Re and the relative roughness $\frac{k}{D}$.

For $\mathrm{Re} \leq 50000$ the difference between (3.48) and (3.49) is less then 1.96% (see Figure 3.5).
We manage the whole range of Reynolds numbers by combining (3.46), (3.47) and (3.49) as follows

$$f = -\frac{\lambda_f}{8}\frac{S}{A}v|v|\left[\frac{N}{kg}\right], \tag{3.50}$$

where λ_f will be given by

$$\lambda_f = \begin{cases} \frac{64}{\mathrm{Re}} & \text{if } \mathrm{Re} \leq \mathrm{Re}_K \\ \\ 1.02(\log \mathrm{Re})^{-2.5} & \text{if } \mathrm{Re} > \mathrm{Re}_K. \end{cases} \tag{3.51}$$

At critical Reynolds number Re_K, we switch the formulae. Any number between 2300 and 4000 can be chosen as mentioned above for the rigid channel. For the flexible part we use the experimental value Re_K proposed in ([1]) $Re_K = 1067$. The dependence of numerical results on the choice of Re_K is discussed in Section 6.5.
We use the following form of the Reynolds number Re

$$\mathrm{Re} = \frac{|v|A}{\nu D_0}, \tag{3.52}$$

which corresponds to the fact that the tube collapses nonsymetrically. We note that this choice increases the frictional losses. This choice also changes the formula for determining the frictional losses in the laminar regime, which was derived from formula (3.45) using (3.42). In this work we neglect this difference.

3.4.2 Tube law

Up to now we derived the balance of mass (3.22) and the balance of momentum (3.34) for three unknowns - the velocity v, the cross-sectional area A and the pressure p. The system is not closed. In this Section we will add an equation decribing the behaviour of the visco-elastic tube.
The simplest form often used in literature is

$$p - p_e = \frac{8hE}{3D_0} \left[\left(\frac{A(x,t)}{A_0} \right)^{\frac{1}{2}} - 1 \right], \tag{3.53}$$

where
p_e is the external pressure,
h is the thickness of the tube,
E is the Young modulus of the tube material,
D_0 is the diameter of the tube in an undeformed state.

The formula (3.53) determines the response of the tube to an arbitrary pressure distribution $p(x)$ and is derived from the linear elasticity theory. In

many papers other versions of (3.53) are used. These formulae are mainly derived from the experimental data. For example the exponent in (3.53) for the real biological materials is bigger than $\frac{1}{2}$.
All such formulae could be written in the form

$$p - p_e = \Phi\left(\frac{A(x,t)}{A_0}\right), \tag{3.54}$$

where Φ is the increasing function; Φ is negative for $A < A_0$ and positive for $A > A_0$. It comes from the fact that if $p - p_e \leq 0$ the tube is compressed and the equilibrium value of A is less then A_0 and vice versa.
In this thesis we deal with the following form of Φ proposed by Shapiro (see [2])

$$\Phi\Big(\frac{A}{A_0}\Big) = \begin{cases} K_P\left[1 - \left(\frac{A}{A_0}\right)^{-\frac{3}{2}}\right] & \text{for the collapsed state } 0 < A \ \leq A_0 \\ \\ -K_E\left(1 - \frac{A}{A_0}\right) & \text{for the inflated state } A_0 < A \end{cases}. \tag{3.55}$$

The formula (3.54) has some disadvantages:

1. cross-sectional area $A(x,t)$ reacts immediately to pressure changes – the time persistence is neglected,
2. (3.53) neglects the longitudinal tensile stress.

Add 1. : We change (3.53) as follows

$$p - p_e = \Phi\left(\frac{A(x,t)}{A_0}\right) + \gamma\frac{\partial}{\partial t}A(x,t). \tag{3.56}$$

We suppose that $x = x_0$, x_0 is an arbitrary position from $\langle 0, l\rangle$. Let us suppose that at time $t = 0$ the pressure p changes from the value p_1 to p_2, futhermore, let us deal with the case that $p_2 > p_1$. The response of the tube will be delayed by the relaxation time τ (see Figure 3.6). We derive a simple formula for time τ.
The equation (3.56) becomes an ordinary differential equation. Moreover, we suppose

$$p(t) - p_e = p_1 \quad \text{for} \quad t < 0, \tag{3.57}$$

$$p(t) - p_e = p_2 \quad \text{for} \quad t \geq 0, \tag{3.58}$$

$$\frac{\partial}{\partial t}A(x_0,t) = 0 \quad \text{for} \quad t < 0. \tag{3.59}$$

It implies that

$$\frac{A(x_0,t)}{A_0} = \Phi^{-1}(p_1 - p_e) \quad \text{for} \quad t < 0. \tag{3.60}$$

(from above mentioned assumptions the function Φ^{-1} exists). The equation (3.56) has, under above assumptions, a continuous solution, so (3.60) is valid also for $t = 0$. We can write at time $t = 0$

$$p_2 - p_1 = \gamma \frac{\partial}{\partial t} A(x_0, 0). \tag{3.61}$$

$$\tag{3.62}$$

From Figure 3.6 yields

$$\frac{\partial}{\partial t} A(x_0, 0) = \frac{A_2 - A_1}{\tau} = \frac{\Phi^{-1}(p_2) - \Phi^{-1}(p_1)}{\tau}, \tag{3.63}$$

and finally we obtain

$$\tau = \gamma \frac{\Phi^{-1}(p_2) - \Phi^{-1}(p_1)}{p_2 - p_1}. \tag{3.64}$$

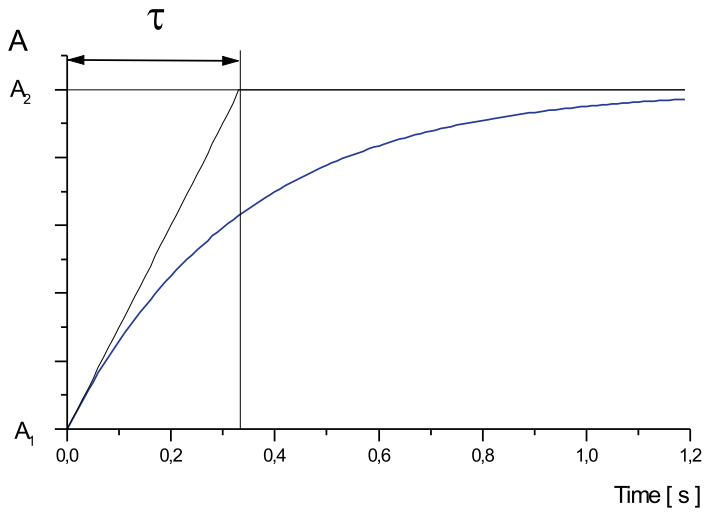

Figure 3.6: The response of the tube to the pressure increment $p_2 - p_1$ at $x = x_0$.

Add 2. : On the left side of (3.53) we add the term representing the tensile stress force. We take two arbitrary material points of the tube and we assume their original positions as on Figure 3.7. (We have no other possibility

since the cross-sectional area $A(x,t)$ contains all the information about the positions of the tube points [independent from y]). We derive the relative deformation in x direction e

$$e = \frac{dS' - dS}{dS} = \frac{\sqrt{h^2 + (\frac{\partial A}{\partial x})^2} - h}{h} = \\ = \frac{\sqrt{1 + \frac{\partial A}{\partial x}^2}}{1} - 1 \doteq 1 + \frac{1}{2}\left(\frac{\partial A}{\partial x}\right)^2 - 1 = \frac{1}{2}\left(\frac{\partial A}{\partial x}\right)^2. \tag{3.65}$$

Using the Hooke law we obtain the tensile stress τ_{xx}

$$\tau_{xx} = Ee, \tag{3.66}$$

and the force acting in x-direction F^x is given by

$$F^x = \frac{\partial}{\partial x}\tau_{xx} = E\frac{\partial A}{\partial x}\frac{\partial^2 A}{\partial x^2}. \tag{3.67}$$

This force F^x is the x-component of the force $\mathbf{F}$, which acts in the normal direction at the surface (see Figure 3.7). Using

$$\frac{\partial A}{\partial x} = \frac{F^x}{F^y}, \tag{3.68}$$

we obtain

$$F^y = E\frac{\partial^2 A}{\partial x^2}. \tag{3.69}$$

After this simple analysis we take the term representing the tensile force in the form

$$\frac{T(E)}{D_0}\frac{\partial^2 A}{\partial x^2}, \tag{3.70}$$

where T(E) is the constant with linear dependence on the Young modulus E. The final form of the tube law is the following

$$\frac{T}{D_0}\frac{\partial^2}{\partial x^2}A(x,t) + p(x,t) - p_e = \Phi\left(\frac{A(x,t)}{A_0}\right) + \gamma\frac{\partial}{\partial t}A(x,t). \tag{3.71}$$

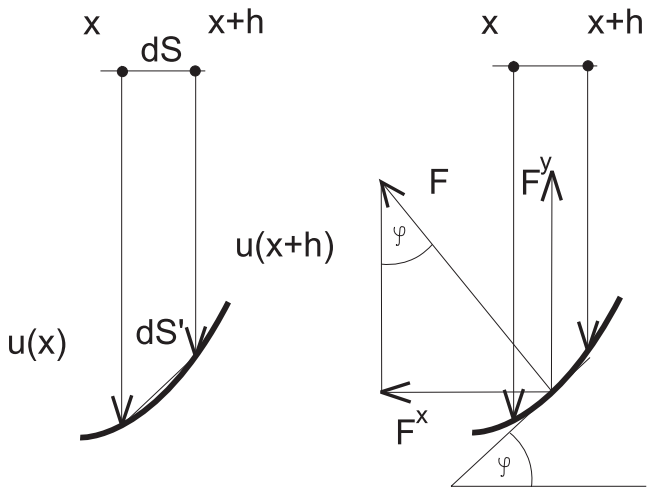

Figure 3.7: The derivation of the tensile stress force

3.5 The viscosity and density of the blood

In this work we deal with the flow in the middle and large vessels (inner diameter $\geq$ 3mm, see Section 2.1.3). In such diameters the blood behaves like a Newtonian fluid. The viscosity depends mainly on the hematocrit H (see Chapter 2.2) and the temperature T. The Figure 3.8 contains the dependence of the viscosity of the blood relatively to the viscosity of water on the hematocrit H at the temperature $T = 37\,^{\circ}C$. The normal values of the hematocrit is given in the Table 3.8. We will take the value $\nu = 4.5{\cdot}10^{-6}[\mathrm{m}^2\mathrm{s}^{-1}]$. The dependence of the viscosity on the temperature is the following - if the temperature decreases by $1^{\circ}C$, the viscosity increases by 2% ([9]).
The density of the blood is $\rho = 1058\,\mathrm{kg\ m}^{-3}$ $(T = 37\,^{\circ}C)$ ([9]).

3.6 The complete system

For the flexible part we have the system

$$\frac{\partial}{\partial t}A(x,t) + \frac{\partial}{\partial x}(A(x,t)v(x,t)) = 0, \tag{3.72}$$

$$\frac{\partial}{\partial t}v(x,t) + v(x,t)\frac{\partial}{\partial x}v(x,t) + \frac{1}{\rho}\frac{\partial}{\partial x}p(x) = -\frac{\lambda_f}{8}\frac{S_0}{A}v|v|, \tag{3.73}$$

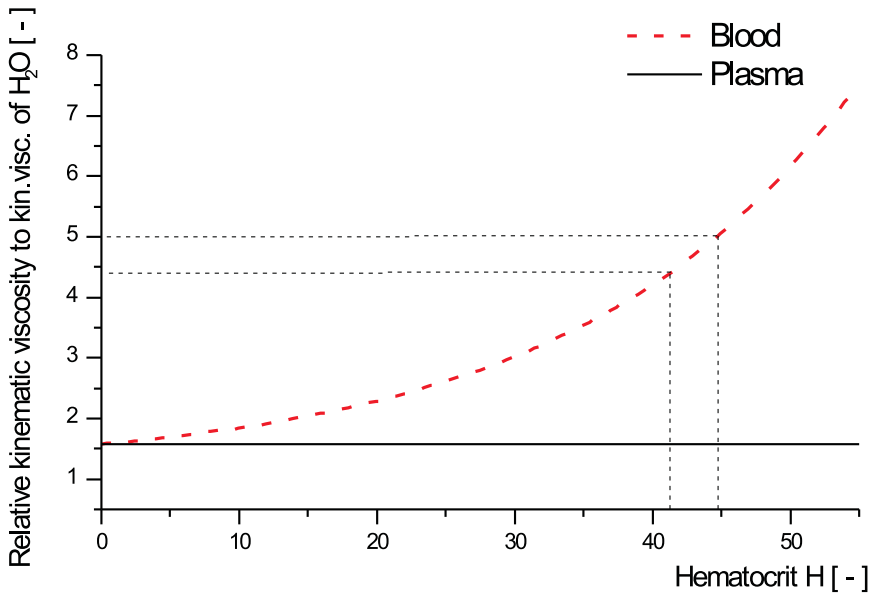

Figure 3.8: The relative kinematic blood viscosity ν to kinematic viscosity of H_2O as a function of hematocrit. The graph was measured by viscosimeter at the temperature $T = 37\,^{\circ}C$.

$$\frac{T}{D_0}\frac{\partial^2}{\partial x^2}A(x,t) + p(x,t) - p_e = \Phi\left(\frac{A(x,t)}{A_0}\right) + \gamma\frac{\partial}{\partial t}A(x,t), \tag{3.74}$$

where

$$\lambda_f = \begin{cases} \frac{64}{\mathrm{Re}} & \text{if } \mathrm{Re} \le \mathrm{Re}_K \\ \\ 1.02(\log \mathrm{Re})^{-2.5} & \text{if } \mathrm{Re} > \mathrm{Re}_K \end{cases}, \tag{3.75}$$

and Re is the local Reynolds number defined by

$$\mathrm{Re} = \frac{|v|A}{\nu D_0}. \tag{3.76}$$

The function Φ is given by

$$\Phi\left(\frac{A}{A_0}\right) = \begin{cases} K_P\left[1 - \left(\frac{A}{A_0}\right)^{-\frac{3}{2}}\right] & \text{for the collapsed state } 0 < A \le A_0 \\ \\ -K_E\left(1 - \frac{A}{A_0}\right) & \text{for the inflated state } A_0 < A \end{cases} \tag{3.77}$$

The equations of motion in rigid parts are

$$\frac{dv_u}{dt} = \frac{p_I - p_u}{\rho l_u} - \frac{\lambda_f}{8}\frac{S_0}{A_0}v_u|v_u|, \tag{3.78}$$

$$\frac{dv_d}{dt} = \frac{p_d - p_E}{\rho l_d} - \frac{\lambda_f}{8}\frac{S_0}{A_0}v_d|v_d|. \tag{3.79}$$

The boundary conditions are given by the following relations

$$p_S = p_I + \frac{1}{2}\rho v_u^2, \tag{3.80}$$

$$p_E = RA_0^2 v_d|v_d|, \tag{3.81}$$

futhermore, the following condition must be satisfied at the junctions of the flexible tube and rigid channels

$$A(0,t) = A(l,t) = A_0. \tag{3.82}$$

The system of equations (3.72)-(3.82) will be denoted by (SYST1).

Remark 2

We are dealing with the pressure drop condition, which is the natural condition. We also could prescribe the fixed velocity v at the inlet, but it would imply that we prescribe the fixed flux $Q = Av$ at the inlet and it is physically impossible, because if the real tube collapses the resistance in the tube increases and the flux in the whole system decreases.

3.7 The two equation system

We derive a simpler model then the model (SYST1). Using the tube law in the form of (3.54)-(3.55) instead of (3.71), it is possible to put the tube law directly into the momentum equation (3.34). Instead of equations (3.72)-(3.74) we obtain the following equations

$$\frac{\partial}{\partial t}A(x,t) + \frac{\partial}{\partial x}(A(x,t)v(x,t)) = 0 \tag{3.83}$$

$$\frac{\partial}{\partial t}v(x,t) + v(x,t)\frac{\partial}{\partial x}v(x,t) + \frac{1}{\rho}\frac{\partial}{\partial x}\Phi\left(\frac{A(x,t)}{A_0}\right) = -\frac{\lambda_f}{8}\frac{S_0}{A}v|v|. \tag{3.84}$$

All the other equations will remain the same. The system of equations (3.83), (3.84) and (3.75)-(3.82) will be denoted by (SYST2).

The system (SYST2) is less realistic, but it is more suitable for theoretical analysis. Because the set of equations (3.83), (3.84) in the system (SYST2) is the hyperbolic system (the set of equations (3.72), (3.73) and (3.74) in the system (SYST1) is not the hyperbolic system in the sense of definition in Appendix 7.2), it is possible to determine its characteristics. We will calculate them in Chapter 4.

Chapter 4

The characteristics of the two equation system

In this Section we calculate characteristics of equations (3.83)-(3.83). We write them down

$$\frac{\partial}{\partial t}A(x,t) + \frac{\partial}{\partial x}(A(x,t)v(x,t)) = 0, \tag{4.1}$$

$$\frac{\partial}{\partial t}v(x,t) + v(x,t)\frac{\partial}{\partial x}v(x,t) + \frac{1}{\rho}\frac{\partial}{\partial x}\Phi\left(\frac{A(x,t)}{A_0}\right) = -\frac{\lambda_f}{8}\frac{S}{A}v|v|. \tag{4.2}$$

The calculation of characteristics is discussed more in Appendix 7.3. We denote the vector of solution by $\mathbf{w} = (A, v)$. We linearize the equations (4.1), (4.2) at the unknown value of the solution (A_0, v_0). From (7.32) follows

$$\frac{\partial}{\partial t}\mathbf{w} + B\frac{\partial}{\partial x}\mathbf{w} = \mathbf{f}, \tag{4.3}$$

where

$$B = \begin{pmatrix} v_o & A_0 \\ \frac{1}{\rho}\frac{\partial\Phi(\frac{A}{A_0})}{\partial A}\Big|_{A=A_0} & v_0 \end{pmatrix}, \quad \mathbf{f} = \begin{pmatrix} 0 \\ -\frac{\lambda_f}{8}\frac{S}{A}v|v| \end{pmatrix},$$

As mentioned in Appendix 7.3 characteristics of the system (4.3) are described by the parameter $\lambda_i = \frac{dt}{dx}, \quad i = 1, 2$. The parameters λ_i are eigen values of the matrix B. We obtain

$$\det\begin{pmatrix} v_o - \lambda & A_0 \\ \frac{1}{\rho}\frac{\Phi(\frac{A}{A_0})}{A}\Big|_{A=A_0} & v_0 - \lambda \end{pmatrix} = (v_0 - \lambda)^2 - \frac{A_0}{\rho}\frac{\partial\Phi(\frac{A}{A_0})}{\partial A}\Big|_{A=A_0} = 0$$

$$\Rightarrow \quad \lambda_{1,2} = v_0 \pm \sqrt{\frac{A_0}{\rho}\frac{\partial\Phi(\frac{A}{A_0})}{\partial A}\Big|_{A=A_0}}.$$

We have obtained two characteristics. The parameter $\lambda_i, i = 1, 2$ represents the speed of the wave propagation in the tube. Because the term $\sqrt{\frac{A_0}{\rho}\frac{\partial\Phi(\frac{A}{A_0})}{\partial A}\Big|_{A=A_0}}$ is usually bigger than the fluid velocity v, the waves propagate in both directions; i.e. in the downstream and upstream directions.

4.1 The wave character of the two equation system

In this Section we briefly discuss the wave character of the equations (4.1), (4.2). We linearize the equations at the values of the solution (A_0, v_0) to obtain the system (4.3). Moreover, we assume that locally the solution of the system could be written in the form

$$\begin{aligned} A(x,t) &= A_0 + \triangle A(x,t); \quad \triangle A(x,t) \ll A_0, \\ v(x,t) &= v_0 + \triangle v(x,t); \quad \triangle v(x,t) \ll v_0. \end{aligned}$$

Neglecting the frictional losses i.e. $\lambda_f = 0$ we have a system

$$\begin{pmatrix} \frac{\partial\triangle A}{\partial t} \\ \\ \frac{\partial\triangle v}{\partial t} \end{pmatrix} + \begin{pmatrix} v_o & A_0 \\ \\ \frac{1}{\rho}\frac{\partial\Phi(\frac{A}{A_0})}{\partial A}\Big|_{A=A_0} & v_0 \end{pmatrix} \begin{pmatrix} \frac{\partial\triangle A}{\partial x} \\ \\ \frac{\partial\triangle v}{\partial x} \end{pmatrix} = \begin{pmatrix} 0 \\ \\ 0 \end{pmatrix}.$$

Moreover we assume:

1. the system (4.1) has sufficiently smooth solution,
2. $v_0 \approx 0$.

We arrive at

$$\frac{\partial\triangle A}{\partial t} + A_0\frac{\partial\triangle v}{\partial x} = 0, \tag{4.4}$$

$$\frac{\partial\triangle v}{\partial t} + \frac{1}{\rho}\frac{\partial\Phi(\frac{A}{A_0})}{\partial A}\Big|_{A=A_0}\frac{\partial\triangle A}{\partial x} = 0. \tag{4.5}$$

If we derivate the equation (4.4) with respect to x, multiply it by $\frac{1}{\rho}\frac{\partial\Phi(A/A_0)}{\partial A}\Big|_{A=A_0}$ and subtract the equation (4.5) derivatived with respect to t we obtain the wave equation for fluctuations $\triangle v$

$$\frac{\partial^2\triangle v}{\partial t^2} - \frac{A_0}{\rho}\frac{\partial\Phi(\frac{A}{A_0})}{\partial A}\Big|_{A=A_0}\frac{\partial^2\triangle v}{\partial x^2} = 0. \tag{4.6}$$

If we derivate the equation (4.4) with respect to t and subtract the equation (4.5) derivatived with respect to x multiplied by A_0 we obtain the wave equation for fluctuations $\triangle A$

$$\frac{\partial^2\triangle A}{\partial t^2} - \frac{A_0}{\rho}\frac{\partial\Phi(\frac{A}{A_0})}{\partial A}\Big|_{A=A_0}\frac{\partial^2\triangle A}{\partial x^2} = 0. \tag{4.7}$$

Here the term

$$c = \sqrt{\frac{A_0}{\rho}\frac{\partial\Phi(\frac{A}{A_0})}{\partial A}\Big|_{A=A_0}} \tag{4.8}$$

is the sound velocity in the tube. We observe that for $v \approx 0$ and small fluctuations the linearized system (4.1) splits into two wave equations (4.6), (4.7).

Chapter 5

Numerical methods

The flow in the flexible and rigid tube setting, see Figure 3.1, is described by the set of equations (3.72)-(3.82) in Section 3.6. We solve this system numerically by the following numerical schemes

1. the so-called simple implicit scheme for flow problems proposed by Patankar ([3]),
2. the Euler implicit scheme,
3. the Crank-Nicholson implicit scheme, and
4. the fractional step scheme.

All schemes are implicit in time, since they are less restrictive in numerical stability and they guarantee the conservation of mass and momentum at each time step.
In Sections 5.1 and 5.2 the system of equations (3.72)-(3.82) is transformed to new variables, the newly created system (5.12) - (5.21) is solved by the methods mentioned above. The Section 5.3 introduces the grid, which is common for all schemes. The simple implicit scheme is derived in Section **??**, the Euler and Crank-Nicholson schemes are discussed in Section 5.4 and the last Section 5.6 is devoted to the fractional step scheme.

5.1 Conversion to Q, A, p variables

The system of equations (3.72)-(3.82) is transformed from v, A, p variables to Q, A, p variables, where Q is the flux given by $Q = Av$. The equation (3.72)

is rewritten as follows

$$\frac{\partial A}{\partial t} + \frac{\partial Q}{\partial x} = 0. \tag{5.1}$$

The equation (3.73) yields

$$\frac{1}{A}\frac{\partial Q}{\partial t} - \frac{Q}{A^2}\frac{\partial A}{\partial t} + \frac{Q}{A}\Big(\frac{1}{A}\frac{\partial Q}{\partial x} - \frac{Q}{A^2}\frac{\partial A}{\partial x}\Big) + \frac{1}{\rho}\frac{\partial p}{\partial x} + \frac{\lambda_f S}{8}\frac{Q|Q|}{A^3} = 0, \tag{5.2}$$

multiplying by A we get

$$\frac{\partial Q}{\partial t} - \frac{Q}{A}\Big(\frac{\partial A}{\partial t} - \frac{\partial Q}{\partial x}\Big) - \frac{Q^2}{A^2}\frac{\partial A}{\partial x} + \frac{A}{\rho}\frac{\partial p}{\partial x} + \frac{\lambda_f S}{8}\frac{Q|Q|}{A^2} = 0. \tag{5.3}$$

Denoting

$$F_T := \frac{\lambda_f S}{8}, \tag{5.4}$$

and using the continuity equation (5.1) to the second term, we have

$$\frac{\partial Q}{\partial t} + 2\frac{Q}{A}\frac{\partial Q}{\partial x} - \frac{Q^2}{A^2}\frac{\partial A}{\partial x} + \frac{A}{\rho}\frac{\partial p}{\partial x} + F_T\frac{Q|Q|}{A^2} = 0. \tag{5.5}$$

The tube law (3.74), and formulae (3.75), (3.77) and (3.82) remain unchanged. Formula (3.76) is transformed into

$$\mathrm{Re} = \frac{|Q|}{\nu D_0}. \tag{5.6}$$

The equations (3.78)-(3.81) are as follows

$$\frac{dQ_u}{dt} = \frac{A_0}{\rho l_u}(p_I - p_u) - F_T\frac{Q_u|Q_u|}{A_0^2}, \tag{5.7}$$

$$\frac{dQ_d}{dt} = \frac{A_0}{\rho l_d}(p_d - p_E) - F_T\frac{Q_d|Q_d|}{A_0^2}, \tag{5.8}$$

$$p_I = p_S - \frac{\rho}{2}\frac{Q_u^2}{A_0^2}, \tag{5.9}$$

$$p_E = RQ_d|Q_d|. \tag{5.10}$$

5.2 Transformation of variables

To keep variables near one during numerical computing, we introduce new variables

$$\begin{aligned} \widetilde{p} &= \frac{p}{p_S}, \\ \widetilde{Q} &= \frac{Q}{Q_0}, \\ \widetilde{A} &= \frac{A}{A_0}, \end{aligned} \tag{5.11}$$

where $\widetilde{p}$, $\widetilde{Q}$, $\widetilde{A}$ are nondimensional quantities. We rewrite the system (5.1) - (5.10)

$$\frac{\partial \widetilde{A}}{\partial t} + \frac{Q_0}{A_0}\frac{\partial \widetilde{Q}}{\partial x} = 0, \tag{5.12}$$

$$\frac{\partial \widetilde{Q}}{\partial t} + 2\frac{Q_0}{A_0}\frac{\widetilde{Q}}{\widetilde{A}}\frac{\partial \widetilde{Q}}{\partial x} - \frac{Q_0}{A_0}\frac{\widetilde{Q}^2}{\widetilde{A}^2}\frac{\partial \widetilde{A}}{\partial x} + p_S\frac{A_0}{Q_0}\frac{\widetilde{A}}{\rho}\frac{\partial \widetilde{p}}{\partial x} + F_T\frac{|Q_0|}{A_0^2}\frac{\widetilde{Q}|\widetilde{Q}|}{\widetilde{A}^2} = 0. \tag{5.13}$$

The F_T is given by (5.4)

$$F_T = \frac{\lambda_f S}{8}, \tag{5.14}$$

and (3.75)

$$\lambda_f = \begin{cases} \frac{64}{\mathrm{Re}} & \text{if } \mathrm{Re} \le \mathrm{Re}_K \\ \\ 1.02(\log \mathrm{Re})^{-2.5} & \text{if } \mathrm{Re} > \mathrm{Re}_K \end{cases}, \tag{5.15}$$

where the Reynolds number is now rewritten

$$\mathrm{Re} = \frac{|Q_0||\widetilde{Q}|}{\nu D_0}, \tag{5.16}$$

and

$$\frac{TA_0}{D_0}\frac{\partial^2 \widetilde{A}}{\partial x^2} = -p_S\widetilde{p} + p_e + \Phi(\widetilde{A}) + \gamma A_0\frac{\partial \widetilde{A}}{\partial t}, \tag{5.17}$$

$$\Phi(\widetilde{A}) = \begin{cases} K_P\left[1 - \widetilde{A}^{-\frac{3}{2}}\right] & \text{for the collapsed state } 0 < \widetilde{A} \le 1 \\ \\ -K_E\left(1 - \widetilde{A}\right) & \text{for the inflated state } 1 < \widetilde{A} \end{cases}, \tag{5.18}$$

$$\frac{d\widetilde{Q}_u}{dt} = \frac{A_0}{Q_0\rho l_u}(p_S - \frac{\rho}{2}\frac{Q_0^2}{A_0^2}\widetilde{Q}_u^2 - p_S\widetilde{p}_u) - F_T\frac{|Q_0|}{A_0^2}\widetilde{Q}_u|\widetilde{Q}_u|, \tag{5.19}$$

$$\frac{d\widetilde{Q}_d}{dt} = \frac{A_0}{Q_0\rho l_d}(p_S\widetilde{p}_d - RQ_0|Q_0|\widetilde{Q}_d|\widetilde{Q}_d|) - F_T\frac{|Q_0|}{A_0^2}\widetilde{Q}_d|\widetilde{Q}_d|. \tag{5.20}$$

By (3.82),

$$\widetilde{A}(0,t) = \widetilde{A}(l,t) = 1. \tag{5.21}$$

The system of equations (5.12) - (5.21) is actually solved by the following numerical algoritmus.

5.3 Grid

Here we introduce the staggered grid used in all schemes. The grid is constructed with N for flow $\widetilde{Q}$ and $N-1$ nodes for cross-sectional area $\widetilde{A}$ and pressure $\widetilde{p}$. The mesh size h is given by

$$h = \frac{l}{N-1}. \tag{5.22}$$

The $\widetilde{A}$- and $\widetilde{p}$-nodes are shifted by half mesh size $\frac{h}{2}$ to the right. The $\widetilde{A}$- and $\widetilde{p}$-nodes are denoted by

$$x_i = \frac{h}{2} + (i-1)h \quad i = 1, \ldots, N-1. \tag{5.23}$$

The values of cross-sectional area $\widetilde{A}$ and pressure $\widetilde{p}$ evaluated in the point x_i are denoted by A_i and p_i respectively. The $\widetilde{Q}$-nodes are denoted by

$$y_i = (i-1)h \quad i = 1, \ldots, N, \tag{5.24}$$

and the value of flux $\widetilde{Q}$ evaluated in the point y_i is denoted by Q_i. The Q_1 and Q_N are the values of the flux at the beginning and end of the flexible part, respectively. Moreover, Q_1 and Q_N represent the average values in the connected rigid parts.

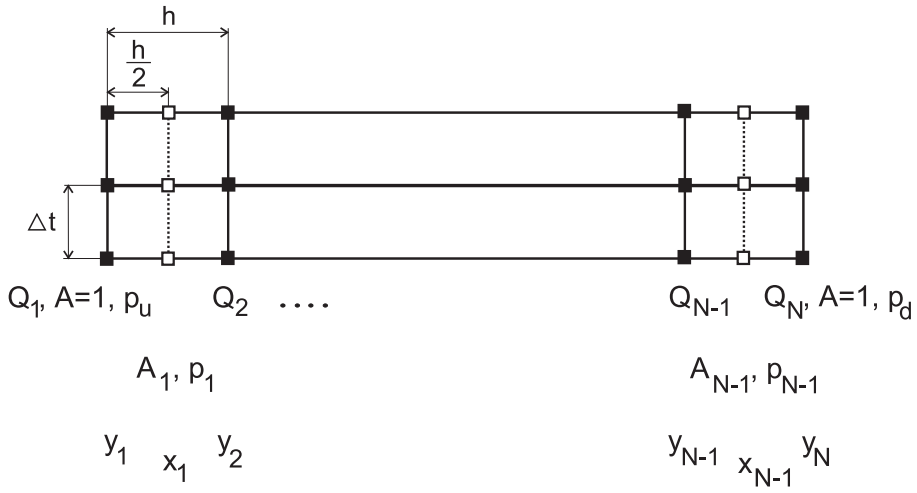

Figure 5.1: The grid system.

5.4 Euler and Crank-Nicholson implicit scheme

We use the grid introduced in Section 5.3. The system of equations (5.12), (5.13), (5.17), (5.19) and (5.20) will be discretized by finite differences. The newly created system of nonlinear algebraic equations will be solved iteratively on each time level. Firstly, to derive this system, we begin with equation (5.17).

Discretization of the equation (5.17)

For $i = 2, \cdots, N-2$ the term $\partial^2 \widetilde{A}/\partial x^2$ is discretized in the common way (the subscript $._i$ denotes the spatial node, in which the term is evaluated):

$$\left.\frac{\partial^2 \widetilde{A}}{\partial x^2}\right|_{x=x_i} = \frac{A_{i-1} - 2A_i + A_{i+1}}{h^2} + O(h^3). \tag{5.25}$$

At $i = 1$ we will find the discretization formula. Due to Figure 5.2 and using the Taylor theorem for sufficiently smooth function we have

$$A_2 = A_1 + h\left.\frac{\partial A}{\partial x}\right|_{x=x_1} + \frac{h^2}{2}\left.\frac{\partial^2 \widetilde{A}}{\partial x^2}\right|_{x=x_1} + O(h^3), \tag{5.26}$$

$$1 = A_1 - \frac{h}{2}\left.\frac{\partial A}{\partial x}\right|_{x=x_1} + \frac{1}{2}\left(\frac{h}{2}\right)^2 \left.\frac{\partial^2 \widetilde{A}}{\partial x^2}\right|_{x=x_1} + O(h^3). \tag{5.27}$$

The last equation multiplyied by 2 and added to equation (5.26)

$$2 - 3A_1 + A_2 = \frac{3}{4}h^2 \frac{\partial^2 \widetilde{A}}{\partial x^2}\Big|_{x=x_1} + O(h^3), \tag{5.28}$$

so the final formula becomes

$$\frac{\partial^2 \widetilde{A}}{\partial x^2}\Big|_{x=x_1} = \frac{8 - 12A_1 + 4A_2}{3h^2} + O(h^3). \tag{5.29}$$

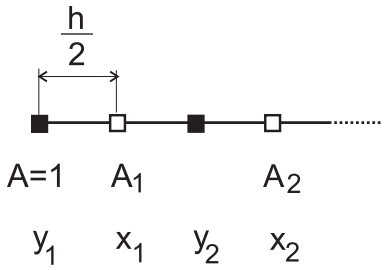

Figure 5.2: To the derivation of the term $\frac{\partial^2 \widetilde{A}}{\partial x^2}\Big|_{x=x_1}$

For the point $i = N - 1$ we can approximate analogously

$$\frac{\partial^2 \widetilde{A}}{\partial x^2}\Big|_{x=x_{N-1}} = \frac{4A_{N-2} - 12A_{N-1} + 8}{3h^2} + O(h^3). \tag{5.30}$$

The time derivative $\partial \widetilde{A}/\partial t$ for $i = 1, \ldots, N-1$ is discretized in the common way

$$\frac{\partial \widetilde{A}}{\partial t}\Big|_{x=y_i} = \frac{A_i - \widehat{A}_i}{\triangle t} + O(\triangle t^2). \tag{5.31}$$

Now we are ready to discretize equation (5.17) ($\widehat{\cdot}$ will denote value from the previous time step)

$$\begin{aligned}
\frac{TA_0}{D_0 h^2}\frac{8 - 12A_1 + 4A_2}{3} &= -p_S p_1 + p_e + \Phi(A_1) + \frac{\gamma A_0}{\triangle t}(A_1 - \widehat{A}_1), \\
\frac{TA_0}{D_0 h^2}(A_{i-1} - 2A_i + A_{i+1}) &= -p_S p_i + p_e + \Phi(A_i) + \frac{\gamma A_0}{\triangle t}(A_i - \widehat{A}_i) \\
&\qquad\qquad i = 2, \ldots, N-2, \\
\frac{TA_0}{D_0 h^2}\frac{4A_{N-2} - 12A_{N-1} + 8}{3} &= -p_S p_{N-1} + p_e + \Phi(A_{N-1}) \\
&\quad + \frac{\gamma A_0}{\triangle t}(A_{N-1} - \widehat{A}_{N-1}).
\end{aligned} \tag{5.32}$$

So finally

$$
\begin{aligned}
C_1 = \frac{TA_0}{D_0 h^2},\ C_2 = \frac{\gamma A_0}{\triangle t},& \\
-(4C_1 + C_2)A_1 + \frac{4}{3}C_1 A_2 &= -\frac{8}{3}C_1 - p_S p_1 + p_e + \Phi(A_1) - C_2\widehat{A}_1, \\
C_1 A_{i-1} - (2C_1 + C_2)A_i + C_1 A_{i+1} &= -p_S p_i + p_e + \Phi(A_i) - C_2\widehat{A}_i \\
& \qquad\qquad i = 2, \ldots, N-2, \\
\frac{4}{3}C_1 A_{N-2} - (4C_1 + C_2)A_{N-1} &= -\frac{8}{3}C_1 + p_e - p_S p_{N-1} + \Phi(A_{N-1}) \\
& \quad - C_2\widehat{A}_{N-1}. \qquad (5.33)
\end{aligned}
$$

We have obtained the system of $N-1$ nonlinear algebraic equations.

Discretization of equations (5.13), (5.19) and (5.20)

To use equations (5.19) and (5.20) we have to express values $\widetilde{p}_u$ and $\widetilde{p}_d$. We calculate these pressures $\widetilde{p}_u$, $\widetilde{p}_d$ with the help of values $p_1, \ldots, p_{N-1}$

$$\widetilde{p}_u = p_1 + \frac{p_1 - p_2}{h}\frac{h}{2} = \frac{3}{2}p_1 - \frac{1}{2}p_2, \qquad (5.34)$$

$$\widetilde{p}_d = p_{N-1} + \frac{p_{N-1} - p_{N-2}}{h}\frac{h}{2} = \frac{3}{2}p_{N-1} - \frac{1}{2}p_{N-2}. \qquad (5.35)$$

We express time derivative of $\widetilde{Q}$ for $i = 1, \ldots, N$ as follows ($\widehat{\cdot}$ denotes value from the previous time step)

$$\left.\frac{\partial \widetilde{Q}}{\partial t}\right|_{x=y_i} = \frac{Q_i - \widehat{Q}_i}{\triangle t} + O(\triangle t^2), \qquad (5.36)$$

Then, using $Q_1 \equiv \widetilde{Q}_u$, $Q_N \equiv \widetilde{Q}_d$, (5.19) and (5.20) yield

$$
\begin{aligned}
\frac{Q_1 - \widehat{Q}_1}{\triangle t} &= \frac{A_0}{Q_0 \rho l_u}\left[p_S - \frac{\rho}{2}\frac{Q_0^2}{A_0^2}Q_1^2 - p_S\left(\frac{3}{2}p_1 - \frac{1}{2}p_2\right)\right] \\
&\quad - \frac{|Q_0|F_T}{A_0^2}Q_1|Q_1|, \qquad (5.37) \\
\frac{Q_N - \widehat{Q}_N}{\triangle t} &= \frac{A_0}{Q_0 \rho l_d}\left[p_S\left(\frac{3}{2}p_{N-1} - \frac{1}{2}p_{N-2}\right)\right. \\
&\quad \left. - RQ_0|Q_0|Q_N|Q_N|\right] - \frac{|Q_0|F_T}{A_0^2}Q_N|Q_N|. \qquad (5.38)
\end{aligned}
$$

So finally

$$Q_1 = \widehat{Q}_1 + \frac{A_0}{Q_0}\frac{\triangle t p_S}{\rho l_u} - \frac{\triangle t}{2l_u}\frac{Q_0}{A_0}Q_1^2 - \frac{A_0}{2Q_0}\frac{p_S \triangle t}{\rho l_u}(3p_1 - p_2) - \frac{\triangle t |Q_0| F_T}{A_0^2} Q_1 |Q_1|, \tag{5.39}$$

$$Q_N = \widehat{Q}_N + \frac{A_0}{Q_0}\frac{\triangle t p_S}{2\rho l_d}(3p_{N-1} - p_{N-2}) - \frac{R A_0 \triangle t |Q_0|}{\rho l_d} Q_N |Q_N| - \frac{\triangle t |Q_0| F_T}{A_0^2} Q_N |Q_N|. \tag{5.40}$$

Now we continue with equation (5.13). We discretize the spatial derivatives for $i = 2, \ldots, N-1$ in $\widetilde{Q}$-nodes

$$\left.\frac{\partial \widetilde{Q}}{\partial x}\right|_{x=y_i} = \frac{Q_{i+1} - Q_{i-1}}{2h} + O(h^2), \ \left.\frac{\partial \widetilde{A}}{\partial x}\right|_{x=y_i} = \frac{A_i - A_{i-1}}{h} + O(h^2),$$

and we approximate value of $\widetilde{A}$ at $\widetilde{Q}$-nodes, see Figure 3.1

$$A_{im} := A_i \approx \frac{A_i + A_{i-1}}{2}. \tag{5.41}$$

Equation (5.13) yields

$$\frac{Q_i - \widehat{Q}_i}{\triangle t} + 2\frac{Q_0}{A_0}\frac{Q_i}{A_{im}}\frac{Q_{i+1} - Q_{i-1}}{2h} - \frac{Q_0}{A_0}\frac{Q_i^2}{A_{im}^2}\frac{A_i - A_{i-1}}{h} + \\ + \frac{A_0}{Q_0}\frac{p_S A_{im}}{\rho}\frac{p_i - p_{i-1}}{h} + \frac{|Q_0| F_T}{A_0^2}\frac{Q_i |Q_i|}{A_{im}^2} = 0 \quad i = 2, \ldots, N-1. \tag{5.42}$$

Multiplying by $\triangle t$ and denoting $\lambda = \triangle t / h$ we have

$$Q_i + \lambda \frac{Q_0}{A_0}\frac{Q_i}{A_{im}}(Q_{i+1} - Q_{i-1}) - \lambda \frac{Q_0}{A_0}\left(\frac{Q_i}{A_{im}}\right)^2 (A_i - A_{i-1}) + \\ + \lambda \frac{A_0}{Q_0}\frac{p_S A_{im}}{\rho}(p_i - p_{i-1}) + \triangle t \frac{|Q_0|}{A_0^2} F_T \frac{Q_i |Q_i|}{A_{im}^2} = \widehat{Q}_i \quad i = 2, \ldots, N-1. \tag{5.43}$$

Equations (5.39), (5.40) and (5.43) create the system of N nonlinear algebraic equations.

Discretization of equations (5.12)

The continuity equation (5.12) will be discretized as follows.
We consider that we are on the new time level and we want to compute values

of Q_i, A_i, p_i. The values from the previous time step will be denoted by $\widehat{\cdot}$. The spatial derivative of $\widetilde{Q}$ is evaluated in $\widetilde{A}$-nodes as follows

$$\left.\frac{\partial \widetilde{Q}}{\partial x}\right|_{x=y_i} = \frac{Q_{i+1} - Q_i}{h} + O(h^2) \quad i = 1, \ldots, N-1, \tag{5.44}$$

and the time derivative of A is evaluated as follows

$$\left.\frac{\partial \widetilde{A}}{\partial t}\right|_{x=y_i} = \frac{A_i - \widehat{A}_i}{\triangle t} + O(\triangle t^2) \quad i = 1, \ldots, N-1. \tag{5.45}$$

We arrive at the system

$$A_i + \frac{Q_0}{A_0}\lambda(Q_{i+1} - Q_i) = \widehat{A}_i \quad i = 1, \ldots, N-1. \tag{5.46}$$

We have now obtained the systems (5.33), (5.39), (5.40), (5.43), and (5.46). We rewrite them in the following way

$$\begin{aligned}
-C_2(A_1 - \widehat{A}_1) + F_1(\mathbf{w}) &= 0, \\
-C_2(A_i - \widehat{A}_i) + F_i(\mathbf{w}) &= 0 \quad i = 1, \ldots, N-1, \\
-C_2(A_{N-1} - \widehat{A}_{N-1}) + F_{N-1}(\mathbf{w}) &= 0, \\
\frac{Q_1 - \widehat{Q}_1}{\triangle t} + F_N(\mathbf{w}) &= 0, \\
\frac{Q_i - \widehat{Q}_i}{\triangle t} + F_i(\mathbf{w}) &= 0 \quad i = N+1, \ldots, 2N-2, \\
\frac{Q_N - \widehat{Q}_N}{\triangle t} + F_{2N-1}(\mathbf{w}) &= 0, \\
A_i - \widehat{A}_i + F_i(\mathbf{w}) &= 0 \quad i = 2N, \ldots, 3N-2,
\end{aligned} \tag{5.47}$$

where

$$\mathbf{w} = (Q_1, A_1, p_1, Q_2, \ldots, Q_{N-1}, A_{N-1}, p_{N-1}, Q_N)$$

is the solution vector. We note that the terms, which correspond to the time derivatives, are separated in (5.47). Now we rewrite (5.47) as follows

$$\begin{aligned}
-C_2 A_1 + \theta F_1(\mathbf{w}) &= -(1-\theta)F_1(\widehat{\mathbf{w}}) - C_2\widehat{A}_1, \\
-C_2 A_i + \theta F_i(\mathbf{w}) &= -(1-\theta)F_i(\widehat{\mathbf{w}}) - C_2\widehat{A}_i \quad i = 1, \ldots, N-1, \\
-C_2 A_{N-1} + \theta F_{N-1}(\mathbf{w}) &= -(1-\theta)F_{N-1}(\widehat{\mathbf{w}}) - C_2\widehat{A}_{N-1}, \\
\frac{Q_1}{\triangle t} + \theta F_N(\mathbf{w}) &= -(1-\theta)F_N(\widehat{\mathbf{w}}) + \frac{\widehat{Q}_1}{\triangle t},
\end{aligned}$$

$$\frac{Q_i}{\triangle t} + \theta F_i(\mathbf{w}) = -(1-\theta)F_i(\widehat{\mathbf{w}}) + \frac{\widehat{Q}_i}{\triangle t} \quad i = N+1, \ldots, 2N-2,$$
$$\frac{Q_N}{\triangle t} + \theta F_{2N-1}(\mathbf{w}) = -(1-\theta)F_{2N-1}(\widehat{\mathbf{w}}) + \frac{\widehat{Q}_N}{\triangle t},$$
$$A_i + \theta F_i(\mathbf{w}) = -(1-\theta)F_i(\widehat{\mathbf{w}}) + \widehat{A}_i \quad i = 2N, \ldots, 3N-2, \quad (5.48)$$

where

$$\theta \in \langle 0, 1\rangle$$
$$\widehat{\mathbf{w}} = (\widehat{Q}_1, \widehat{A}_1, \widehat{p}_1, \widehat{Q}_2, \ldots, \widehat{Q}_{N-1}, \widehat{A}_{N-1}, \widehat{p}_{N-1}, \widehat{Q}_N). \quad (5.49)$$

θ is an arbitrary parameter between 0 and 1. For the choice $\theta = 1$ we obtain the Euler scheme, for the choice $\theta = 0.5$ we obtain the Crank-Nicholson scheme. The Euler scheme is the first order accurate in time, the Crank-Nicholson scheme is the second order accurate in time.

Iterative procedure

The nonlinear system of algebraic equations (5.48) is solved by means of the Newton method (see Appendix 7.4). It means that we have to compute the Jacobian matrix of the vector on the left hand side of the system (5.48). As follows from numerical experiments, it is necessary to keep all equations in the same order of magnitude. Therefore, equations in (5.48) for which $i = 1, \ldots, N-1$ are multiplyed by the factor

$$\frac{1}{C_1}, \quad (5.50)$$

where C_1 is defined in (5.33).
To obtain the Jacobian matrix with nonzero elements near diagonal we reorder the system (5.48) as follows

$$\mathbf{u}(\mathbf{w}) + \theta\mathbf{G}(\mathbf{w}) = -(1-\theta)\mathbf{G}(\widehat{\mathbf{w}}) + \widehat{\mathbf{u}}(\widehat{\mathbf{w}}), \quad (5.51)$$

where

$$\mathbf{u} = (\frac{Q_1}{\triangle t}, A_1, -\frac{C_2}{C_1}\ A_1\ , \frac{Q_2}{\triangle t}, A_2, -\frac{C_2}{C_1}A_2, \frac{Q_3}{\triangle t}, \ldots$$
$$\ldots, \frac{Q_{N-1}}{\triangle t}, A_{N-1}, -\frac{C_2}{C_1}A_{N-1}, \frac{Q_N}{\triangle t}), \quad (5.52)$$

$$\mathbf{G} = (F_N, F_{2N}, \frac{F_1}{C_1},\ F_{N+1}\ , F_{2N+1}, \frac{F_2}{C_1}, F_{N+2}, \dots$$
$$\dots, F_{2N-2}, F_{3N-2}, \frac{F_{N-1}}{C_1}, F_{2N-1}). \quad (5.53)$$

The Jacobian matrix is defined as

$$J = \frac{\partial \left(\mathbf{u}(\mathbf{w}) + \theta \mathbf{G}(\mathbf{w})\right)}{\partial \mathbf{w}}. \quad (5.54)$$

The Jacobian matrix has 11 nonzero diagonals.
Now we briefly describe the iterative procedure. We suppose that we have the values on k-th time level and we want to calculate the values on $k+1$-th time level. The following iterative procedure is proceeded on every time level

1. As the first iterative values of the Q_i, A_i, and p_i we take the values from the previous time level $\widehat{Q_i}$, $\widehat{A_i}$, and $\widehat{p_i}$.
2. We solve system (5.51) by means of the Newton method. We stop the iteration process if the residuum res of system (5.51) is less than some limit res_{MAX}

$$res \leq res_{MAX}. \quad (5.55)$$

Each linear iteration is solved by the Gauss elimination method (The choice of linear solver is discussed in Section 6.2). The ω was around 0.7.

5.5 Fractional step scheme

The fractional step scheme is a modification of the schemes introduced in the previous Section. It was first proposed by Glowinski [14]. It is an implicit method, second order accurate in time.
We start from the system of equations (5.49). The Euler and Crank-Nicholson schemes use the fixed time step $\triangle t$ and the parameter θ on every time level. The fractional step scheme uses the different length of the time step $\triangle t_i$ and different values of θ_i on every i-th time level. The values of $\triangle t_i$, θ_i are shown

in the following Table

Fractional step method	$\triangle t_i$	θ_i
1.step	$(1-\frac{1}{\sqrt{2}})3\triangle t$	$\sqrt{2}(\sqrt{2}-1)$
2.step	$(\sqrt{2}-1)3\triangle t$	$\sqrt{2}-1$
3.step	$(1-\frac{1}{\sqrt{2}})3\triangle t$	$\sqrt{2}(\sqrt{2}-1)$
5.step	as in the 1.step	as in the 1.step
6.step	as in the 2.step	as in the 2.step
etc	etc.	etc.

(5.56)

We note that

$$\overline{\triangle t} := \sum_{i=1}^{3} \frac{\triangle t_i}{3} = \triangle t, \tag{5.57}$$

$$\overline{\theta} := \sum_{i=1}^{3} \frac{\theta_i}{3} \sim 0.529. \tag{5.58}$$

so the $\overline{\theta}$ is slightly larger than the corresponding value for the Crank Nicholson scheme $\bar{\theta} = 0.5$. The method has the same accurancy as the Crank Nicholson scheme, but it has better stability properties, it is so-called *strongly stable*.
To clarify this property we look first at the scalar linear equation

$$\dot{x}(t) + \lambda x(t) = 0, \quad t \geq 0, \tag{5.59}$$

where $\lambda \in \mathbf{C}$, $Re\lambda \geq 0$. An arbitrary time stepping scheme applied to this equation, with constant time step size $\triangle t$, generates a sequence of values $x_n \sim x(t_n)$, with $t_n := n\triangle t$. The behaviour of the scheme as $t \to \infty$, depending on the parameter λ, is ussually characterized by the $amplification factor$ $\omega = \omega(\lambda\triangle t)$. The value x_n can be expressed as $x_n = \omega^n x_0$. In terms of ω, we formulate the following desirable properties of time stepping schemes:

1. $|\omega(\lambda\triangle t)| \leq 1$(local stability),
2. $\lim_{Re\lambda\to\infty} |\omega(\lambda\triangle t)| \leq 1 - O(\triangle t)$(stability),
3. $\lim_{Re\lambda\to\infty} |\omega(\lambda\triangle t)| \leq 1 - \delta < 1$(strong stability).

Annalogously we can define these properties for the general linear evolution equation

$$\frac{\partial u}{\partial t} + D(t)u = f(t), \quad D_n = D(t_n), \quad f_n = f(t_n). \tag{5.60}$$

The approximation properties can be expressed in terms of the amplification factor $\omega(\lambda \triangle t)$ with λ eigenvalue of $D(t)$. The fractional step scheme and Euler scheme are strongly stable, the Crank Nicholson scheme is only stable ([13]).
Further, the fractional step scheme contains very little numerical dissipation which is crucial in the computation of self-excited oscillations ([13]). For more details see [13], or [15].
The iterative procedure is the same as in the previous Section.

5.6 Program implementation

The all numerical algoritmus, which mentioned above, as well as linear and nonlinear solvers were implemented in C++ language. The code was programmed using Microsoft Visual C++ 6.0. The code is added on CD-ROM in the directory *Elastic*. The basic linear algebra is implemented in files

math0.h/math0.cpp,

math1.h/math1.cpp,

math2.h/math2.cpp.

The above mentioned numerical schemes you can find in files

knihovna1.h/knihovna1.cpp.

The CD-ROM also includes executable file *elastic.exe* in directory *Elastic/Release* (for the platform Windows 95/98/2000/NT). Read file *readme.txt* for more information. If you plan to use the code ask me for the newest version. I will be glad to give it to you :-)(vitastembera@hotmail.com).

Chapter 6

Numerical results

Here we discuss numerical results of the system (SYST1) (the equations (3.72)-(3.82)). Throughout this Chapter the folllowing values of parameters will be used (unless noted otherwise):

Parameter	**Value**	**Unit**
l	0.1	[m]
l_u	0.15	[m]
l_d	0.15	[m]
D_0	0.01	[m]
p_S[1]	13300	[Pa]
p_e	13000	[Pa]
R	3.10^{11}	[$\mathrm{Pa^2 s^2 m^{-6}}$]
ρ	1058	[kg $\mathrm{m^{-3}}$]
ν	$4.5{\cdot}10^{-6}$	[$\mathrm{m^2 s^{-1}}$]
Re_K	1067	[−]
K_P	5000	[Pa]
K_E	121000	[Pa]
T	2500	[N $\mathrm{m^{-1}}$]
γ	10000	[Pa s $\mathrm{m^{-2}}$]

(6.1)

We note that the graphs presented here represent the flexible part of the tube system (see Figure 3.1), since rigid parts are represented only with one grid point.

6.1 Initial conditions

We choose initial conditions in the form that they satisfy the boundary conditions (5.19), (5.20) and (3.82). We set

$\widetilde{A}(0,x) = 1 \quad [-]$	$A_0 = \frac{\pi}{4} D_0^2 = 0.0000785 \quad [\mathrm{m}^2]$
$\widetilde{Q}(0,x) = 1 \quad [-]$	$Q_0 = 0.0000785$ [3] $\quad [\mathrm{m}^3\mathrm{s}^{-1}]$

(6.2)

so (3.82) is fulfilled. The pressure is choosen in the form

$$p(x) = \frac{l-x}{l} p_u + \frac{x}{l} p_d. \tag{6.3}$$

We rewrite equations (5.19), (5.20). Assuming that $\frac{\mathrm{d}\widetilde{Q}}{\mathrm{dt}} = 0$, (5.19) and (5.20) yield to

$$p_S p_u = p_S - \frac{\rho}{2} - \rho l_u \frac{F_T}{A_0} \tag{6.4}$$

$$p_S p_d = R Q_0^2 + \rho l_d \frac{F_T}{A_0}. \tag{6.5}$$

Using

$$\begin{aligned} \mathrm{Re} &= \frac{Q_0}{\nu D_0} \approx 174 < \mathrm{Re}_K \quad \Rightarrow \lambda_f = \frac{64}{\mathrm{Re}}, \\ \frac{F_T}{A_0} &= \frac{\lambda_f S_0}{8 A_0} = \frac{8 S_0}{\mathrm{Re} A_0} = \frac{32\nu}{Q_0}, \end{aligned} \tag{6.6}$$

and $Q_0 \equiv A_0$ we have finally

$$p_u = \frac{1}{p_S} \left[p_S - \frac{\rho}{2} - \rho l_u \frac{32\nu}{A_0} \right], \tag{6.7}$$

$$p_d = \frac{1}{p_S} \left[R A_0^2 + \rho l_d \frac{32\nu}{A_0} \right]. \tag{6.8}$$

[1] 13.3kPa $\equiv$ 100mmHg.
[3] $I.e. v_0 = 1 m/s$.

6.2 Choice of linear solver

For the Euler, Crank-Nicholson and fractional step methods we solve the system of nonlinear equations by means of the Newton method on every time level. At the every nonlinear iteration of the Newton method we solve the system of linear equations. We have tried two solvers: the direct Gauss elimination and the well known SOR method (Successive overrelaxation method). The Gauss elimination is not often used because it is an extremaly slow method (of order n^3) and it accumulates the rounding error. But from our experiences it is more robust than SOR method. For $N > 12$ approximately the SOR method diverges even for very small parameter omega as illustrated on Figure 6.1. The residuum of the system of linear algebraic equations res is defined as follows (the L^1 norm of a vector is defined by (**??**))

$$res = \|Ax - \mathbf{b}\|_{L^1}. \tag{6.9}$$

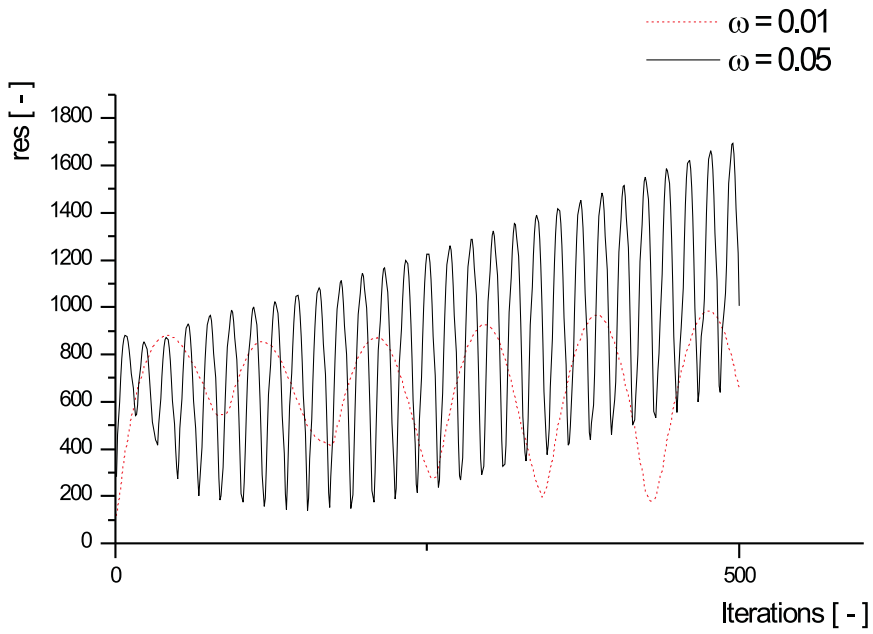

Figure 6.1: The residuum of SOR solver for the different values of ω ($N = 20, \triangle t = 2.5 \cdot 10^{-4}\, s$).

Therefore for the Euler, Crank-Nicholson and fractional step methods we use the Gauss elimination method and for the simple implicit method we use

SOR method. In the future we want to use an iterative method which is more robust, for example BiCGStab (see [17]).

6.3 Test of all methods on rigid channel

All the methods were tested on the rigid channel, which cross-sectional area $\check{A}$ is given by

$$\check{A}(x) = A_0 \left[\frac{1}{2} + \frac{2}{l^2}(x - \frac{l}{2})^2 \right]. \tag{6.10}$$

The code was changed in the following way. We changed the function Φ given by (5.18) as follows

$$\Phi(\widetilde{A}, x) = \begin{cases} K_P \left[1 - \widetilde{A}^{-\frac{3}{2}} \right] \text{ for } 0 < \widetilde{A} < \frac{1}{2} + \frac{2}{l^2}(x - \frac{l}{2})^2 \\ \\ -K_E \left(1 - \widetilde{A} \right) \quad \text{for } \ \frac{1}{2} + \frac{2}{l^2}(x - \frac{l}{2})^2 < \widetilde{A} \end{cases}, \tag{6.11}$$

and constants K_P, K_E were increased 10^5 times. It was sufficient to keep the tube rigid. The initial conditions were taken in the form $A_0(x) = \check{A}(x)$ and $v = 1[m/s]$ i.e. $Q = \check{A}(x)$. After one time step with sufficient number of nonlinear iterations all methods recovered the constant flux Q along the tube.

6.4 Comparing of all methods

First we focus on the fractional step method. The following table contains the convergence parameters for a different number of nodes N, and the time step $\triangle t$. The relaxation parameter for the Newton method (see (7.37)) ω

equals 0.7.

res_{MAX}[5]	**N**	$\triangle t$ [s]	**min.n.of iter.steps**	**max.n.of iter.steps**	**ratio n.of iter.steps**
10^{-2}	20	$2.5{\cdot}10^{-4}$	3	4	3.88
10^{-2}	40	$1.25{\cdot}10^{-4}$	3	4	3.91
10^{-2}	80	$0.625{\cdot}10^{-4}$	3	4	3.91
10^{-4}	20	$2.5{\cdot}10^{-4}$	7	10	8.12
10^{-4}	40	$1.25{\cdot}10^{-4}$	7	9	7.93
10^{-4}	80	$0.625{\cdot}10^{-4}$	7	12	7.88
10^{-6}	20	$2.5{\cdot}10^{-4}$	11	27	14.42
10^{-6}	40	$1.25{\cdot}10^{-4}$	11	26	13.03
10^{-6}	80	$0.625{\cdot}10^{-4}$	11	25	12.04

The Figure 6.2 shows the convergence of the cross-sectional area A at the position $x = 0.075\,m$ for $N = 20$ and $\triangle t = 2.5{\cdot}10^{-4}\,s$.

The Figure 6.3 compares results for different number of nodes N and time steps $\triangle t$.

We compare these results with the situation $K_P = 1400$, $T = 1750$. The following table contains the convergence parameters for a different number of nodes N, and the time step $\triangle t$ for this case

res_{MAX}	**N**	$\triangle t$ [s]	**min.n.of iter.steps**	**max.n.of iter.steps**	**ratio n.of iter.steps**
10^{-2}	20	$2.5{\cdot}10^{-4}$	3	6	4.23
10^{-4}	80	$0.625{\cdot}10^{-4}$	7	18	8.95
10^{-4}	20	$2.5{\cdot}10^{-4}$	7	13	8.24
10^{-4}	40	$1.25{\cdot}10^{-4}$	7	15	8.55
10^{-6}	20	$2.25{\cdot}10^{-4}$	11	18	12.22
10^{-6}	40	$1.25{\cdot}10^{-4}$	11	13	12.27

[5] res_{MAX} is defined by (5.55).

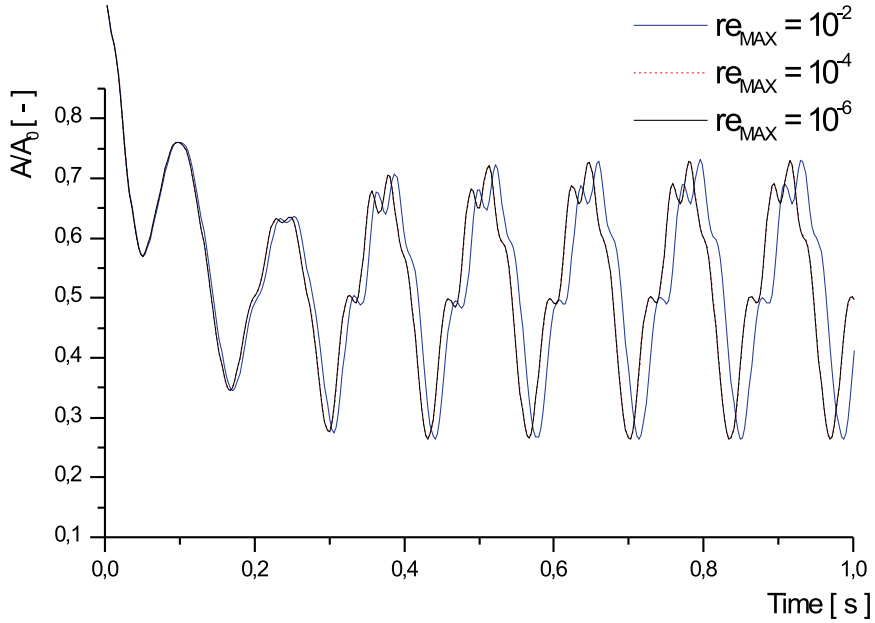

Figure 6.2: The calculation of the cross-sectional area $A(x,t)$ at the position $x = 0.075\,m$ for the different maximal residuum res_{MAX} ($N = 20$, $\triangle t = 2.5 \cdot 10^{-4}\,s$). We note that the graphs for $res_{MAX} = 10^{-4}$ and $res_{MAX} = 10^{-6}$ coincide).

The convergence on the fix grid and fix time step is the same as in the previous case (Figure 6.2). The test of convergence for a different number of nodes N and a different time step $\triangle t$ is shown in Figure 6.4. We see the differenties between graphs for $t \geq 0.3\,s$, we think that it is because of the self-excited oscillattions have not so simple structure as in the previous case and the system is highly sensitive to the change of initial conditions.

In the following we concern with the Crank-Nicholson and Euler methods. The Figure 6.5 clearly shows the first order accurency of the Euler method comparing to the second order accurency of the Crank-Nicholson and fractional step methods. The Figure 6.6 shows that for sufficiently small maximal residuum res_{MAX} we obtain the identical results.

The last method – the simple implicit method is less robust and for the case of nondecreasing oscillations does not converge. We test the method for the parameter $K_P = 5000$, $T = 3000$ and $p_e = 9\,kPa$, when damping oscillations occure.

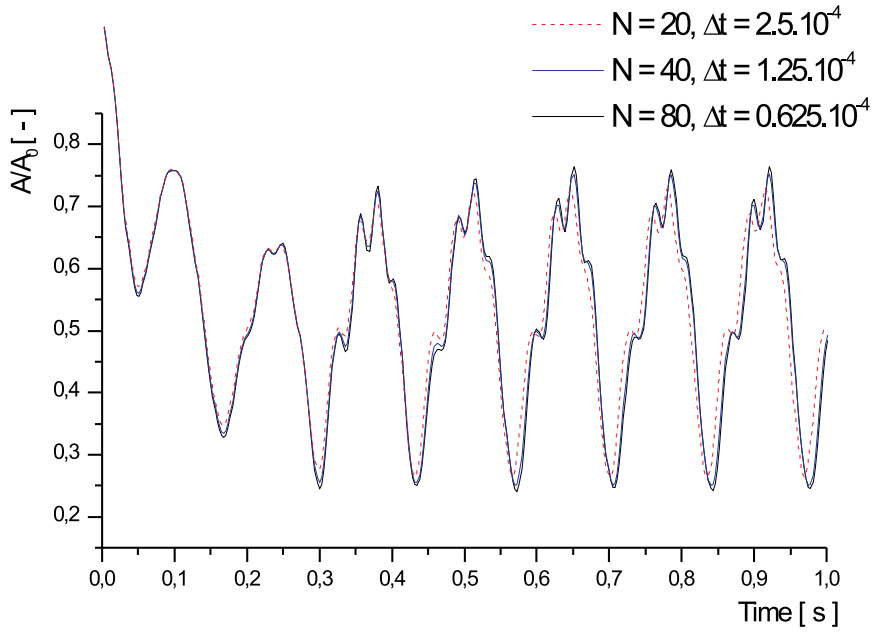

Figure 6.3: The calculation of the cross-sectional area $A(x,t)$ at the position $x = 0.075\,m$ for the different maximum maximum residuum res_{MAX} ($N = 20$, $\triangle t = 2.5 \cdot 10^{-4}\,s$, $res_{MAX} = 10^{-6}$).

6.5 Main results

Further in this Section we use the fractional step method, number of nodes $N = 40$, the time step $\triangle t = 1.25 \cdot 10^{-4}$ and the maximum residuum during nonlinear iterations $res_{MAX} = 10^{-5}$.
We have observed the periodic self-excited oscillations as shown on Figures 6.7, 6.8. Figure 6.7 compares the time dependences of the cross-sectional area A/A_0, pressure p/p_S and the flux Q/Q_0 at the position $x = 0.075m$ on the time. Figure 6.8 compares the dependences of the A/A_0 and the Reynolds number Re on time at the same position. The spatial disributions of the cross-sectional area A/A_0, pressure p/p_S and the flux Q/Q_0 during one time period – at $0\% \equiv 100\%$, at 33% and at 66% of the time period – are illustrated in Figures 6.9, 6.10 and 6.11. (Figures 6.9-6.11 are calculated by the Crank-Nicholson method – the reason is that the fractional step method changes the time step on every time level and it is complicated to obtain the spatial distributions at the concrete three independent time instants.) The frequency of the self-excited oscillations shown in Figures 6.7-6.11 is approximately $7.4\,Hz$.

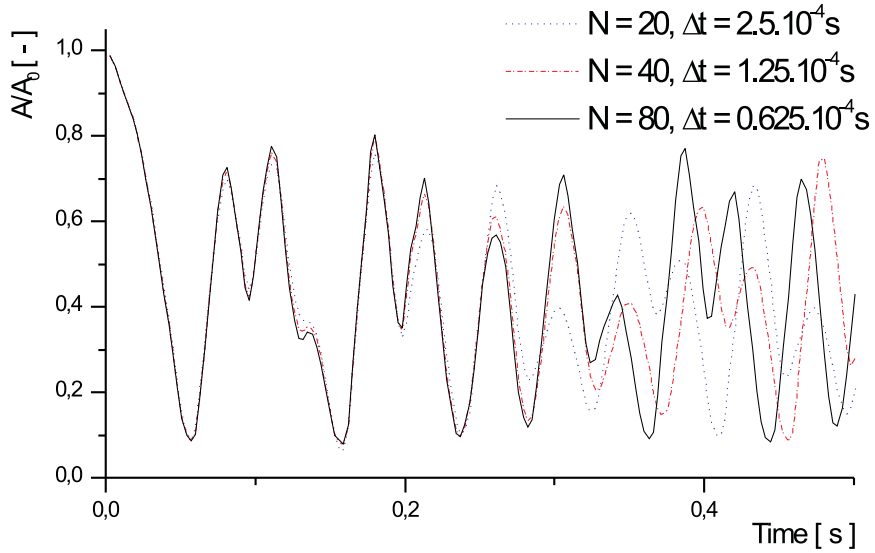

Figure 6.4: The calculation of the cross-sectional area $A(x,t)$ at the position $x = 0.075\,m$ for a different number of nodes N and time step $\triangle t$ ($K_P = 1400$, $T = 1750$, $res_{MAX} = 10^{-6}$).

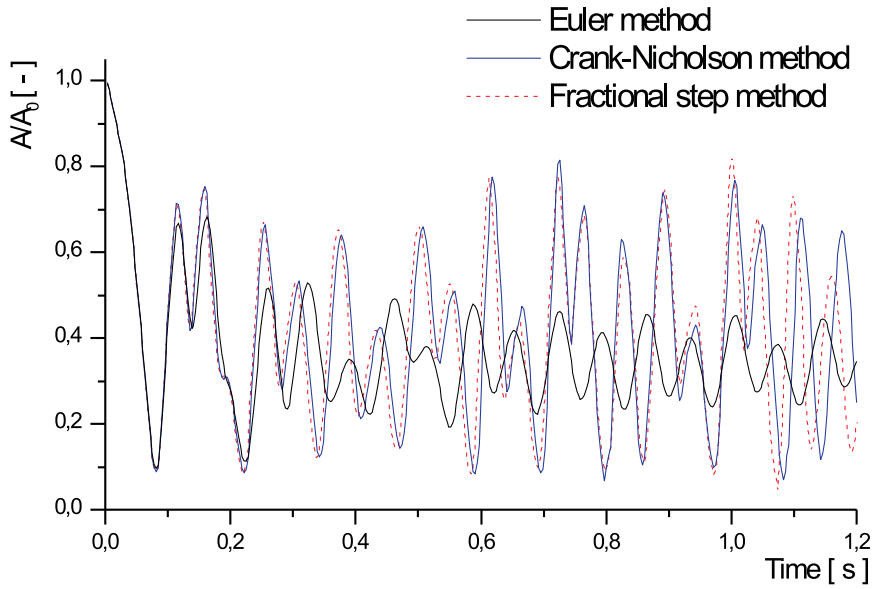

Figure 6.5: The calculation of the cross-sectional area $A(x,t)$ at the position $x = 0.075\,m$ for the different methods ($N = 20$, $\triangle t = 2.5 \cdot 10^{-4}\,s$, $res_{MAX} = 0.5$).

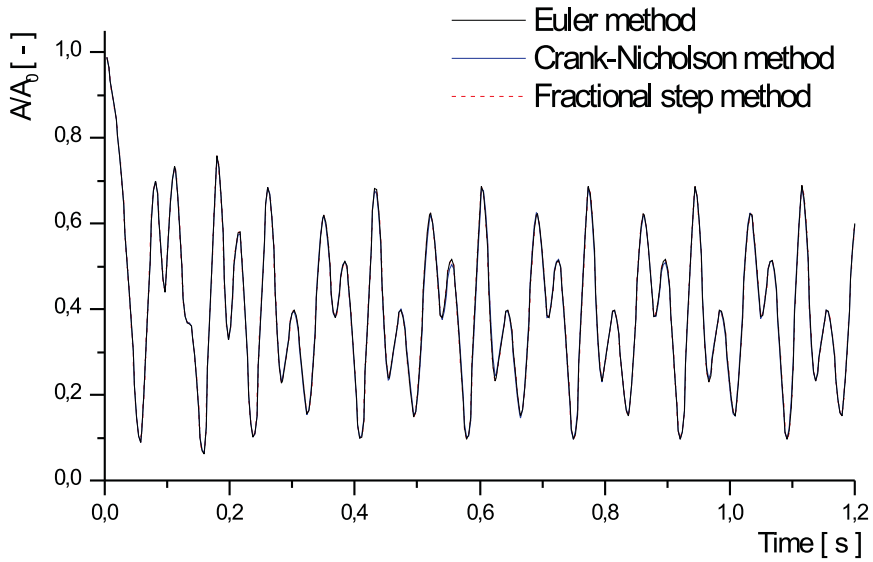

Figure 6.6: The calculation of the cross-sectional area $A(x,t)$ at the position $x = 0.075\,m$ for the different methods ($N = 20$, $\triangle t = 2.5{\cdot}10^{-4}\,s$, $res_{MAX} = 10^{-5}$).

Figure 6.12 shows the dependence of the frequency of the self-excited oscillations on parameter T. Figure 6.13 shows that the influence of the viscous term γ on numerical results is negligible.

In the next text we focus on the influence of the frictional coefficient λ_f given by (3.75) on the self-excited oscillations. Roughly speaking, if the term is big enough the self-excited oscillations occur, if not the tube collapses. The frictional coeficient λ_f is mainly given by the critical Reynolds number Re_K and also by the definition of the Reynold number in the flexible tube (compare equations (3.42), (3.52)). The increasing of Re_K decreases the value of λ_f and tube can collapse as shown in Figure 6.14. This does not hold if the Reynold number Re in the system is too large – for example for the flow illustrated in Figures 6.7 and 6.8 the change of Re_K from 1067 to 2300 has no effect. The choice of the formula (3.42) instead of (3.52) has the same effect – the parameter λ_f decreases and the tube collapses in larger range of parameters.

We also observed the self-excited oscillations with more complicated structure – see Figure 6.15. The system is very sensitive to the initial conditions in this case, see Figure 6.4 in the previous Section.

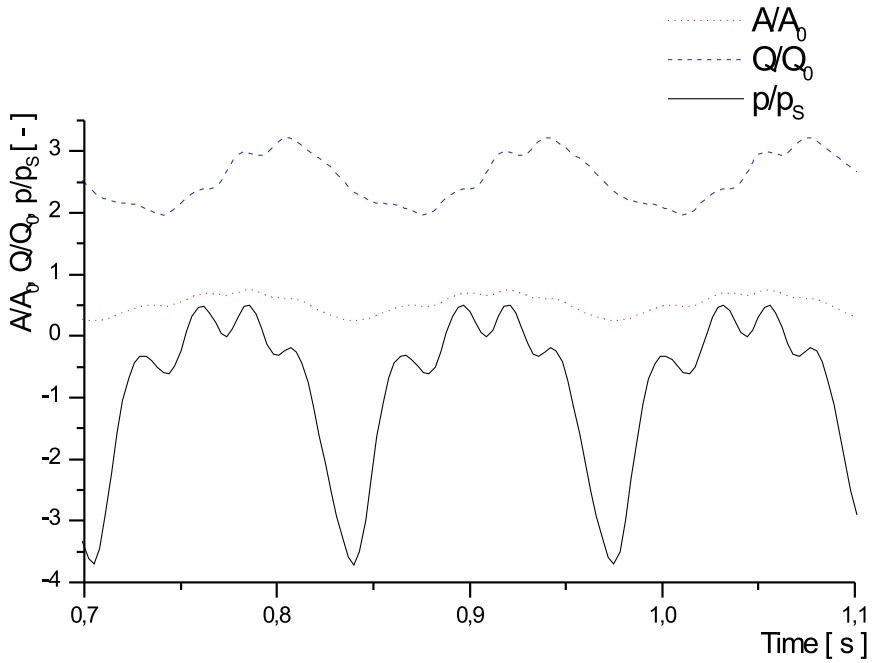

Figure 6.7: The cross-sectional area A/A_0, pressure p/p_S and the flux Q/Q_0 at the position $x = 0.075\,m$ ($K_p = 5000$, $T = 2500$, fractional step method, $N = 40$, $\triangle t = 1.25{\cdot}10^{-4}\,s$, $res_{MAX} = 10^{-5}$).

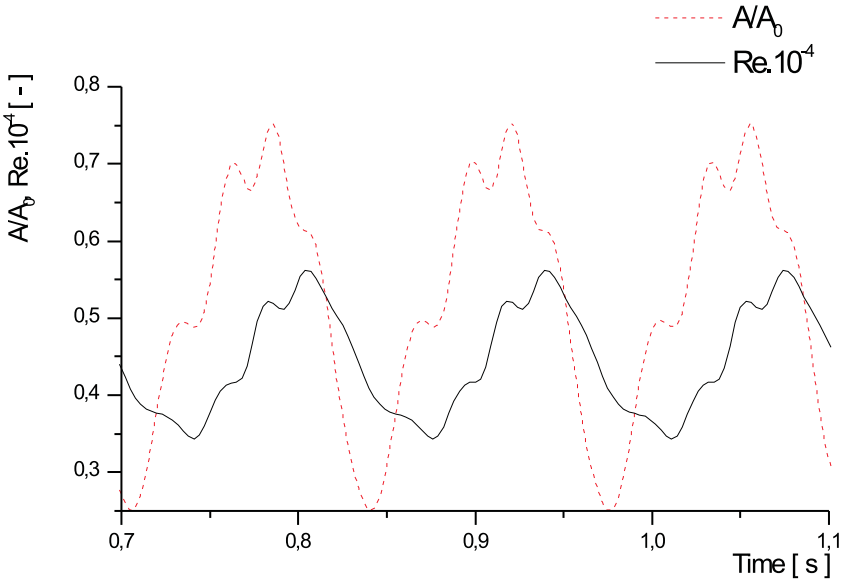

Figure 6.8: The cross-sectional area A/A_0 and the Reynolds number Re at the position $x = 0.075\,m$ ($K_p = 5000$, $T = 2500$, fractional step method, $N = 40$, $\triangle t = 1.25{\cdot}10^{-4}\,s$, $res_{MAX} = 10^{-5}$).

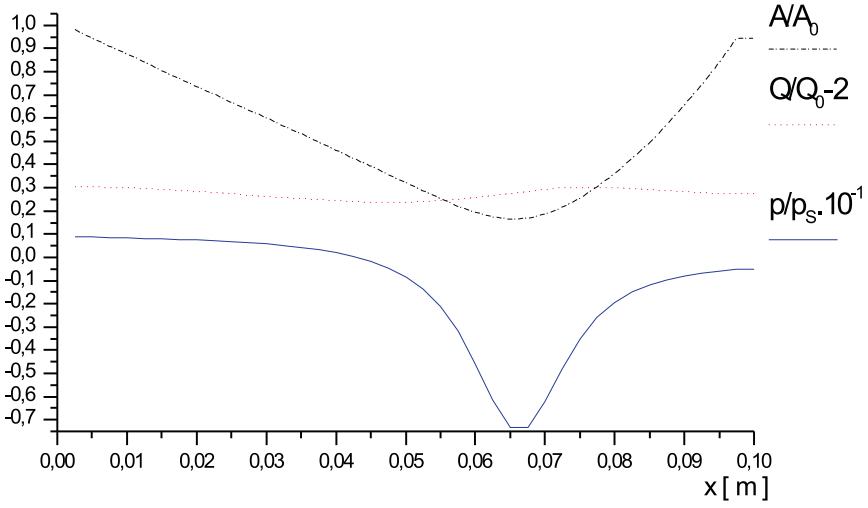

Figure 6.9: The spatial distribution of the cross-sectional area A/A_0, pressure $p/p_S{\cdot}10^{-1}$ and flux $Q/Q_0 - 2$ at the beginning (and at the end) of the time period) ($t = 0.3\,s$ respectively $t = 0.435\,s$). ($K_p = 5000$, $T = 2500$, Crank-Nicholson method, $N = 40$, $\triangle t = 1.25{\cdot}10^{-4}\,s$, $res_{MAX} = 10^{-5}$).

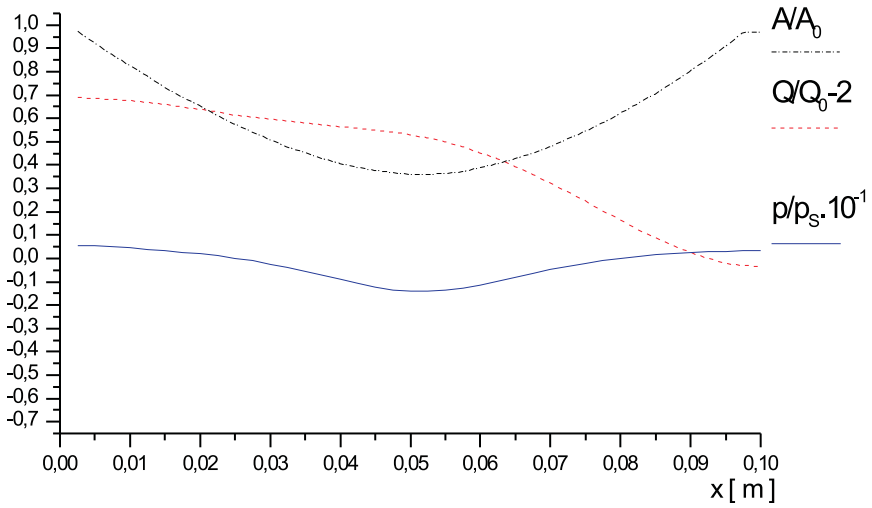

Figure 6.10: The spatial distribution of the cross-sectional area A/A_0, pressure $p/p_S{\cdot}10^{-1}$ and flux $Q/Q_0 - 2$ at one-third of the time period ($t = 0.345\,s$). ($K_p = 5000$, $T = 2500$, Crank-Nicholson method , $N = 40$, $\triangle t = 1.25{\cdot}10^{-4}\,s$, $res_{MAX} = 10^{-5}$).

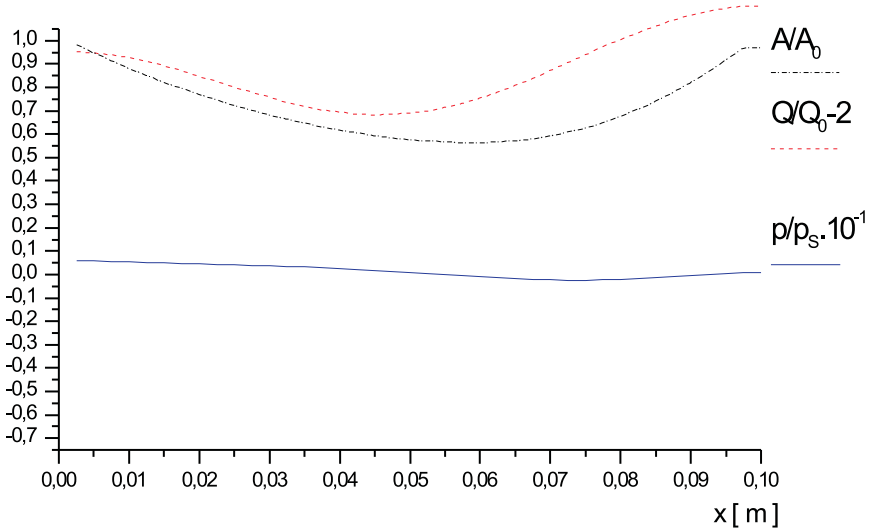

Figure 6.11: The spatial distribution of the cross-sectional area A/A_0, pressure $p/p_S{\cdot}10^{-1}$ and flux $Q/Q_0 - 2$ at second-third of the time period ($t = 0.39\,s$). ($K_p = 5000$, $T = 2500$, Crank-Nicholson method, $N = 40$, $\triangle t = 1.25{\cdot}10^{-4}\,s$, $res_{MAX} = 10^{-5}$).

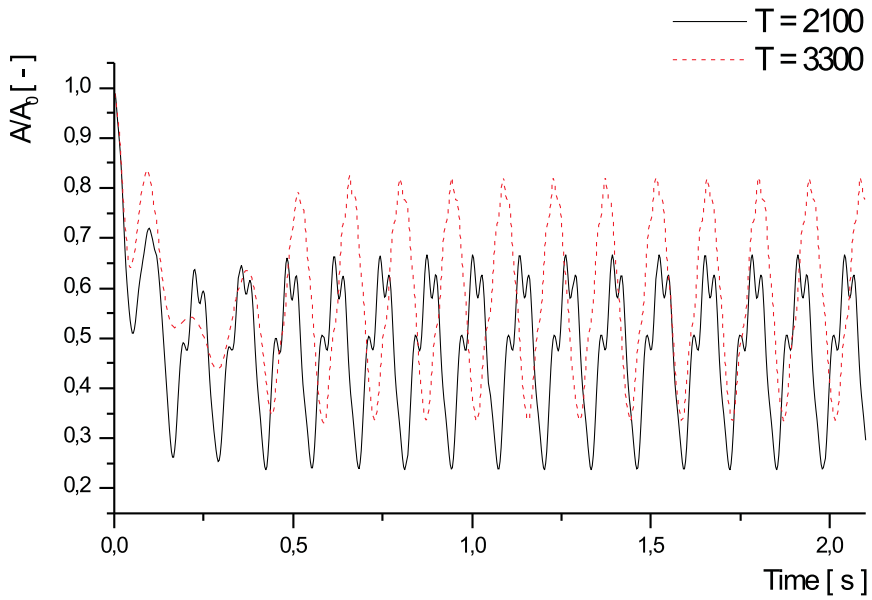

Figure 6.12: Dependence of A/A_0 on T at the position $x = 0.075\,m$ ($K_p = 5000$, fractional step method, $N = 40$, $\triangle t = 1.25{\cdot}10^{-4}\,s$, $res_{MAX} = 10^{-5}$).

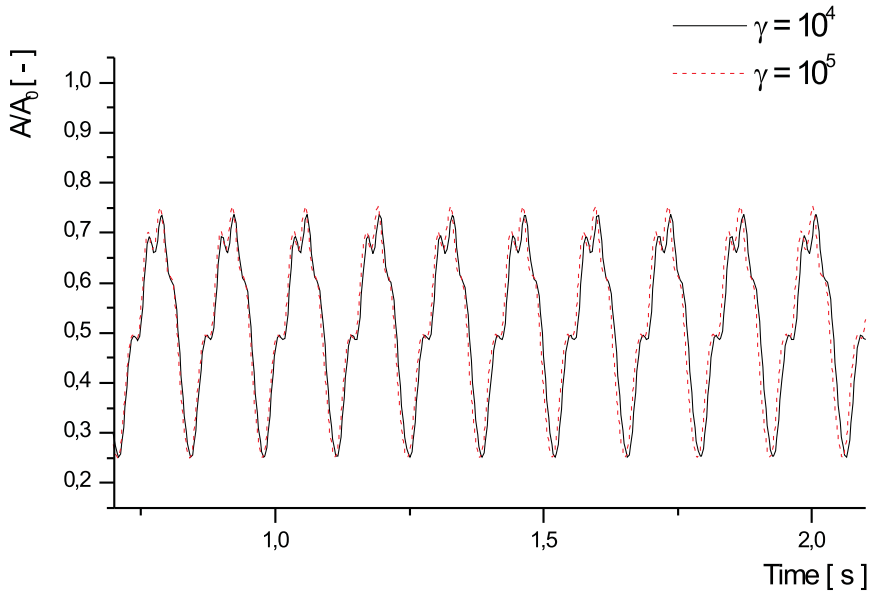

Figure 6.13: Dependence of A/A_0 on γ at the position $x = 0.075\,m$ ($K_p = 5000$, $T = 2500$, fractional step method, $N = 40$, $\triangle t = 1.25{\cdot}10^{-4}$, $res_{MAX} = 10^{-5}$).

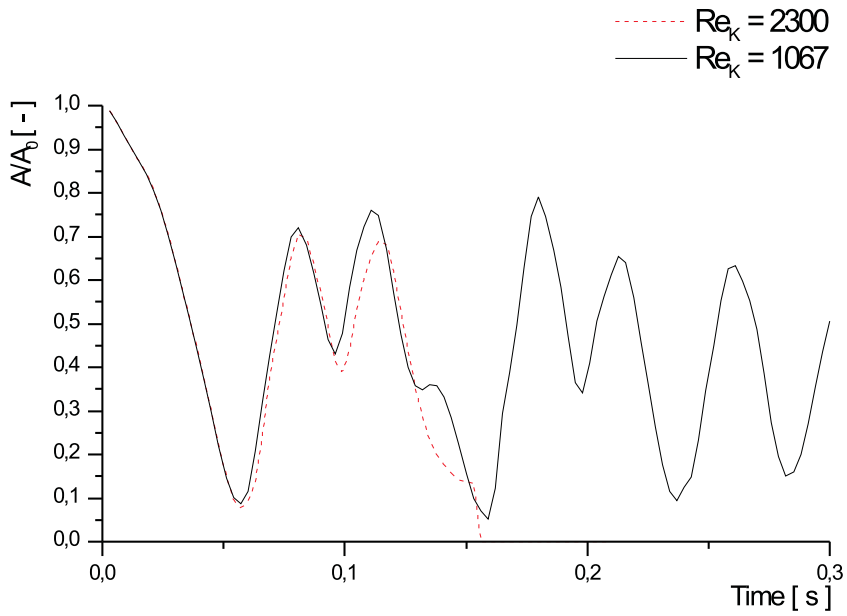

Figure 6.14: The collapse of the tube for the choice of the critical Reynolds number $\mathrm{Re}_K = 2300$ instead of to $\mathrm{Re}_K = 1067$ at the position $x = 0.075\,m$ ($K_p = 5000$, $T = 2500$, fractional step method, $N = 20$, $\triangle t = 1.25{\cdot}10^{-4}\,s$, $res_{MAX} = 10^{-6}$).

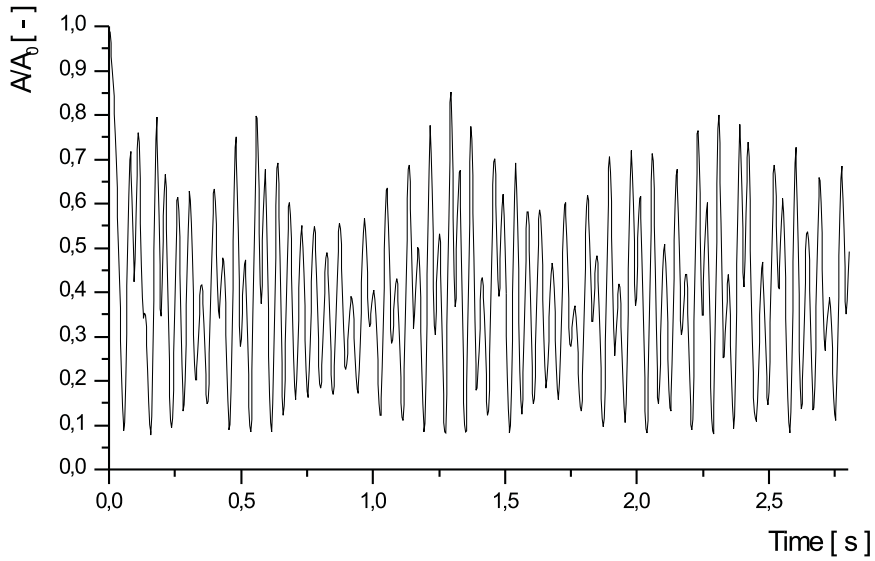

Figure 6.15: The more complicated structure of self-excited oscillations of the cross-sectional area A/A_0 at the position $x = 0.075\,m$ ($K_p = 1400$, $T = 1750$, fractional step method, $N = 40$, $\triangle t = 1.25{\cdot}10^{-4}$, $res_{MAX} = 10^{-5}$).

Chapter 7

Appendix

7.1 Transport theorem

We investigate the motion of fluid occupying the domain V_t at instant $t \in (T_1, T_2)$. We take an arbitrary instant $t_0 \in (T_1, T_2)$ and we assume that the domain V_{t_0} is bounded, with the Lipschitz-continuous boundary. The motion of fluid is described by the function

$$\Upsilon : V_{t_0} \subset \mathbf{R}^3 \times (T_1, T_2) \to V_t \subset \mathbf{R}^3, \quad \mathbf{x} = \Upsilon(\mathbf{X}, t), \quad t \in (T_1, T_2), \quad (7.1)$$

introduced in Section 3.1. Let the function

$$F = F(\mathbf{x}, t) : \mathcal{M} \to \mathbf{R}, \quad (7.2)$$

where $\mathcal{M}$ is defined as

$$\mathcal{M} = \{(\mathbf{x}, t); \mathbf{x} \in V_t, t \in (T_1, T_2)\}, \quad (7.3)$$

be a density of some extensive (see Section 3.2) physical quantity $\mathcal{F}$. Let $\sigma(t_0)$ be an arbitrary volume such that $\overline{\sigma(t_0)} \subset V_{t_0}$, then we define the volume $\sigma(t)$ as

$$\sigma(t) = \{\Upsilon(\mathbf{X}, t) : \mathbf{X} \in V_{t_0}, t \in (T_1, T_2)\}. \quad (7.4)$$

The total amount of the quantity $\mathcal{F}$ in the volume $\sigma(t)$ equals the integral

$$\mathcal{F}(t) = \int_{\sigma(t)} F(\mathbf{x}, t) d\mathbf{x}. \quad (7.5)$$

Then the following theorem holds

Theorem 1 *Let the above mentioned assumptions hold. Futhermore we assume*

- *The mapping* $\Upsilon(\mathbf{X},t), \mathbf{X}=(x_1,X_2,X_3), \mathbf{X}\in\sigma(t_0), t\in(T_1,T_2)$ *has continuous first order derivatives with respect to* t, X_1, X_2, X_3 *and continuous second order derivatives* $\partial^2\Upsilon/\partial t\partial X_i, i=1,2,3$.
- *The mapping* $\mathbf{X}\in\sigma(t_0)\to\mathbf{x}=\Upsilon(\mathbf{X},t)$ *for an arbitrary* $t\in(T_1,T_2)$ *is continuously differentable one-to-one mapping and the Jacobian defined as*

$$J_C(\mathbf{X},t)=\det\left(\frac{\partial\Upsilon}{\partial\mathbf{X}}\right), \tag{7.6}$$

which is contiuous and bounded and satisfy the condition

$$J_C(X,t)>0 \quad \forall X\in\sigma(t_0), \forall t\in(T_1,T_2). \tag{7.7}$$

- *Let the function* $F=F(x,t)$ *have continuous and bounded first order derivatives on set* $\{(x,t); x\in\sigma(t), t\in(T_1,T_2)\}$.

Then for each $t\in(T_1,T_2)$ *there exists a finite derivative*

$$\frac{d}{dt}\mathcal{F}(t)=\int_{\sigma(t)}\left[\frac{\partial F(x,t)}{\partial t}+\operatorname{div}\left(F(x,t)\mathbf{v}(x,t)\right)\right]dx, \tag{7.8}$$

where the operator div *is defined as*

$$\operatorname{div}:=\sum_{i=1}^{3}\frac{\partial}{\partial x_i}. \tag{7.9}$$

Before we proove the theorem we proove the following lemma

Lemma 1 *Let the assumptions of above theorem be satisfied. Then Jacobian* $J_C=J_C(X,t)$ *has a continuous and bounded partial derivative* $\partial J_C/\partial t$ *for* $\mathbf{X}\in\sigma(t_0)$, $t\in(T_1,T_2)$ *and*

$$\begin{aligned}\frac{\partial J_C(\mathbf{X},t)}{\partial t}&=J_C(\mathbf{X},t)\sum_{i=1}^{3}\frac{\partial v_i(\mathbf{x},t)}{\partial x_i},\\ \mathbf{x}&=\Upsilon(\mathbf{X},t).\end{aligned} \tag{7.10}$$

Proof : We expand the Jacobian $J_C(X,t)$ by the i-th row:

$$J_C(\mathbf{X},t) = \sum_{\alpha=1}^{3} \frac{\partial \Upsilon_i}{\partial X_\alpha}(\mathbf{X},t) D_{i,\alpha}(\mathbf{X},t), \tag{7.11}$$

where $D_{i,\alpha}(\mathbf{X},t)$ denotes the cofactor of the element $\partial\Upsilon_i/\partial X_\alpha$. For $\alpha,\beta = 1,2,3$ cofactors $D_{i,\beta}$ are independent of $\partial\Upsilon_i/\partial X_\alpha$. Hence,

$$\frac{\partial J_C}{\partial\left(\partial\Upsilon_i/\partial X_\alpha\right)} = D_{i,\alpha}. \tag{7.12}$$

In order to calculate the derivative $\partial J_C/\partial t$, we consider the determinant $J_C(\mathbf{X},t)$ as a function dependent on the element $\partial\Upsilon_i/\partial X_\alpha$ which depends on t

$$\frac{\partial J_C}{\partial t} = \sum_{i,\alpha=1}^{3} \frac{\partial^2 J_C}{\partial(\partial\Upsilon_i/\partial X_\alpha)} \frac{\partial}{\partial t}\left(\frac{\partial \Upsilon_i}{\partial X_\alpha}\right) = \sum_{i,\alpha=1}^{3} D_{i,\alpha} \frac{\partial^2 \Upsilon_i}{\partial X_\alpha \partial t}. \tag{7.13}$$

Moreover

$$\begin{aligned} \frac{\partial^2 \Upsilon_i}{\partial X_\alpha \partial t}(\mathbf{X},t) &= \frac{\partial^2 \Upsilon_i}{\partial t \partial X_\alpha}(\mathbf{X},t) = \frac{\partial}{\partial X_\alpha} v_i(\Upsilon(\mathbf{X},t),t) = \\ &= \sum_{j=1}^{3} \frac{\partial v_i}{\partial x_j}(\mathbf{x},t) \frac{\partial \Upsilon_j}{\partial X_\alpha}(\mathbf{X},t). \end{aligned} \tag{7.14}$$

Substituting into (7.13), we have

$$\frac{\partial J_C}{\partial t} = \sum_{i,\alpha=1}^{3} D_{i,\alpha} \sum_{j=1}^{3} \frac{\partial \Upsilon_j}{\partial X_\alpha} \frac{\partial v_i}{\partial x_j} = \sum_{i,j=1}^{3} \left(\sum_{\alpha=1}^{3} \frac{\partial \Upsilon_j}{\partial X_\alpha} D_{i,\alpha} \right) \frac{\partial v_i}{\partial x_j}. \tag{7.15}$$

We show that the following equation holds

$$\sum_{\alpha=1}^{3} \frac{\partial \Upsilon_j}{\partial X_\alpha} D_{i,\alpha} = J\delta_{i,j}. \tag{7.16}$$

In the case that $i = j$ it is nothing else then the definition of the determinant of Jacobian matrix J_C. And when $i \neq j$ the left hand side of the equation (7.16) is the determinant of the matrix, with the same two rows (i-th and j-th) and therefore it is zero. So thus we can put (7.16) to (7.15) and we finally obtain

$$\frac{\partial J_C}{\partial t} = J_C \sum_{i,j=1}^{3} \delta_{i,j} \frac{\partial v_i}{\partial x_j} = J_C \sum_{i=1}^{3} \frac{\partial v_i}{\partial x_i} = J_C \mathrm{div}\mathbf{v} \tag{7.17}$$

♠.

Now we are ready to prove the transport theorem

Proof of the theorem : By the substitution theorem, we rewrite the integral (7.5) as follows

$$\mathcal{F}(t) = \int_{\sigma(t_0)} F(\Upsilon(\mathbf{X},t),t) J_C(\mathbf{X},t) d\mathbf{X}. \tag{7.18}$$

Since t_0 is fixed and the integration domain $\sigma(t_0)$ does not depend on time t, we can apply the well-known theorem on differentiation of an integral with respect to a parameter

$$\frac{d\mathcal{F}}{dt} = \int_{\sigma(t_0)} \Big[\left(\frac{\partial F}{\partial t}(\Upsilon(\mathbf{X},t),t) + \sum_{i=1}^{3} \frac{\partial F}{\partial x_i}(\Upsilon(\mathbf{X},t),t) \frac{\partial \Upsilon_i}{\partial t}(\mathbf{X},t) \right) \times$$
$$\times\ J_C(\mathbf{X},t) + F(\Upsilon(\mathbf{X},t),t) \frac{\partial J_C}{\partial t}(\mathbf{X},t) \Big] d\mathbf{X}. \tag{7.19}$$

The assumptions considered guarantee the correctness of the differentiation under the integral sign. In view of lemma 1 and the formula (3.5) we get the identity

$$\frac{d\mathcal{F}}{dt} = \int_{\sigma(t_0)} \Big[\frac{\partial F}{\partial t}(\Upsilon(\mathbf{X},t),t) + \sum_{i=1}^{3} \frac{\partial F}{\partial x_i}(\Upsilon(\mathbf{X},t),t) v_i(\Upsilon(\mathbf{X},t),t) +$$
$$+\ F(\Upsilon(\mathbf{X},t),t) \sum_{i=1}^{3} \frac{\partial v_i}{\partial x_i}(\Upsilon(\mathbf{X},t),t) \Big] J_C(\mathbf{X},t) d\mathbf{X}. \tag{7.20}$$

If we use the inverse substitution, transforming the integral over $\sigma(t_0)$ onto the integral over $\sigma(t)$, we obtain the formula (7.8) ♠.

7.2 Definition of hyperbolic system

The hyperbolic system of partial differential equations in one space dimension is defined as follows

Definition 1 *Let $\mathcal{O} \subset \mathbf{R^s}$ be a domain and let $\mathbf{f}$ be a smooth function from $\mathcal{O}$ into $\mathbf{R^s}$. We say that the system of partial differential equations*

$$\frac{\partial \mathbf{w}}{\partial t} + \frac{\partial \mathbf{f}(\mathbf{w})}{\partial x} = 0 \quad in \quad \mathbf{R}^+ \times \mathbf{R}, \tag{7.21}$$

is hyperbolic *if the Jacobian matrix defined as*

$$J(\mathbf{w}) = \frac{\partial \mathbf{f}}{\partial \mathbf{w}}(\mathbf{w}), \tag{7.22}$$

has the s real eigenvalues and is diagonalizable[1].

The definition of the hyperbolic system in higher dimensions can be found in [16].

7.3 The characteristics of the hyperbolic system in one space dimension

Let us deal for a moment with the linear system of hyperbolic equations in the form

$$\frac{\partial \mathbf{w}}{\partial t} + B\frac{\partial \mathbf{w}}{\partial x} = 0 \quad \text{in} \quad \mathbf{R}^+ \times I, \tag{7.23}$$

where

$$\mathbf{w} = (w_1, w_2, \ldots, w_s),$$

$I \subset \mathbf{R}$ is an open interval and $B \in \mathbf{M}^{s\times s}$ is the diagonalizable matrix with s real eigenvalues (see Definition 1). The characteristic is a curve

$$\zeta(s) = (\zeta^x(s), \zeta^t(s)), \tag{7.24}$$

on which the solution vector $\mathbf{w}$ is constant. This can be written down as

$$d\mathbf{w} = \frac{\partial \mathbf{w}}{\partial t}\zeta^{t'}(s) + \frac{\partial \mathbf{w}}{\partial x}\zeta^{x'}(s) = 0. \tag{7.25}$$

Under the assumption that $\zeta^{t'} \neq 0$ we can define the parameter λ, describing the direction of the characteristic as

$$\lambda(s) = \frac{dx}{dt} = \frac{\zeta^{x'}(s)}{\zeta^{t'}(s)}. \tag{7.26}$$

We obtain

$$\frac{\partial \mathbf{w}}{\partial t} + \lambda(s)\frac{\partial \mathbf{w}}{\partial x} = 0. \tag{7.27}$$

[1]The square matrix A is called diagonalizable if there exists the regular square matrix P, such that $B = P^{-1}AP$, where B is the diagonal matrix.

The equations (7.23), (7.27) create the system of $2s$ linear algebraic equatons for uknowns $\partial w_1/\partial t, \ldots, \partial w_s/\partial t, \partial w_1/\partial x, \ldots, \partial w_s/\partial x$. The system with the zero right side has a nontrivial solution if and only if

$$\det \begin{pmatrix} I & B \\ I & \lambda I \end{pmatrix} = 0 \tag{7.28}$$

$$\iff \det(B - \lambda I) = 0. \tag{7.29}$$

From (7.29) follows that parameters $\lambda_1, \ldots, \lambda_s$ are the eigen values of the matrix B. The characteristics of the system of equations (7.23), (7.27) are lines in $\mathbf{R}^+ \times I$.
Now we focus in the system of the type

$$\frac{\partial \mathbf{w}}{\partial t} + B\frac{\partial \mathbf{w}}{\partial x} = \mathbf{H}(\mathbf{w}) \quad \text{in} \quad \mathbf{R}^+ \times I. \tag{7.30}$$

The characteristics of such system are usually calculated in the same way as written above, but the obtained characteristics do not satisfy the condition (7.25).
Now let us deal with the nonlinear system of the type

$$\frac{\partial \mathbf{w}}{\partial t} + \frac{\partial \mathbf{f}(\mathbf{w})}{\partial x} = \mathbf{H}(\mathbf{w}) \quad \text{in} \quad \mathbf{R}^+ \times I. \tag{7.31}$$

The following heuristic approach is often used. We drop first the right hand side of the equation (7.31). Then we take an arbitrary point $(x_0, t_0) \in \mathbf{R}^+ \times I$, where, for now, the unknown solution has a value $\mathbf{w_0}$. We linearize the system (7.31) at the value $\mathbf{w_0}$ as follows

$$\frac{\partial \mathbf{w}}{\partial t} + J(\mathbf{w_0})\mathbf{w} = 0 \quad \text{in} \quad \mathbf{R}^+ \times I, \tag{7.32}$$

where J is the Jacobian matrix of the mapping $\mathbf{f}$ (see 7.22). We obtain the values $\lambda_1, \ldots, \lambda_s$ by the same technique as mentioned above. The obtained characteristic lines coincide with the characteristics of the system (7.31) locally in the neighbourhood of the point (x_0, t_0). We repeat this procedure for all $(x_0, t_0) \in \mathbf{R}^+ \times I$. i.e. for all values $\mathbf{w_0}$ and we finally obtain the values $\lambda_1(\mathbf{w}), \ldots, \lambda_s(\mathbf{w})$. The signs of the parameters $\lambda_i, i = 1, \ldots, s$ are usually independent from $\mathbf{w}$, which is helpful for determining of the appropriate boundary conditions for the system (7.31). Let us deal with the case that $s = 2$, $\lambda_1 > 0$ and $\lambda_2 < 0$ (see Figure 7.1). The system (7.31) has two characteristics, the first one going to the right and the second one going to the left. The solution propagates in waves and the characteristics determine

the points of the same phase of the wave. Therefore we should prescribe one of the unknowns w_1, w_2 fixed on the left side (the Dirichlet boundary condition) and free on the right side (the Neumann boundary condition) and the second one free on the left side and fixed on the right side.

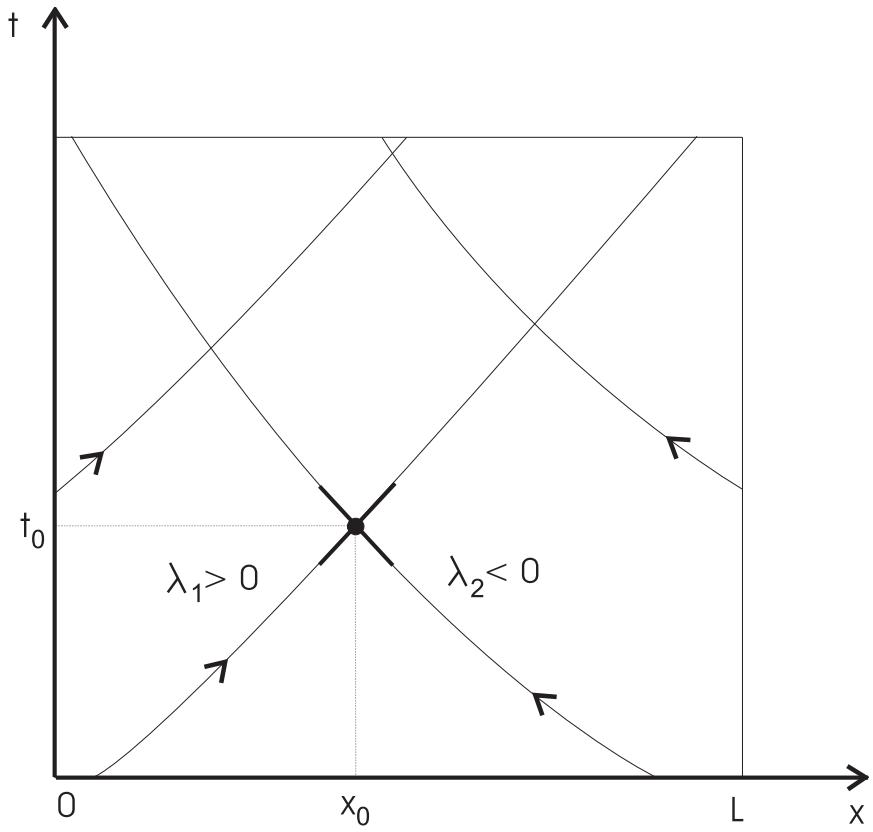

Figure 7.1: The characteristics of the system of two nonlinear hyperbolic equations for the case $\lambda_1 > 0, \lambda_2 < 0$.

7.4 Newton method

The Newton method is the numerical method for solving the system of nonlinear algebraic equations of the form

$$\mathbf{F}(\mathbf{X}) = 0 \quad \text{, where} \quad \mathbf{F} : \mathbf{R^n} \to \mathbf{R^n}. \tag{7.33}$$

The derivation of the method is very simple. We denote the solution of the system (7.33) by $\mathbf{U}$ and we assume that we have the k-th iteration of

the solution $\mathbf{U}^k$. To obtain $(k+1)$-th iteration $\mathbf{U}^k$ we use the Taylor series expansion as follows

$$0 = \mathbf{F}(\mathbf{U}) \sim \mathbf{F}(\mathbf{U}^k) + J(\mathbf{U}^k)(\mathbf{U} - \mathbf{U}^k), \tag{7.34}$$

where J is the Jacobian matrix of the mapping $\mathbf{F}$ defined as

$$J(\mathbf{U}) = \frac{\partial \mathbf{F}}{\partial \mathbf{U}}(\mathbf{U}). \tag{7.35}$$

Putting $\mathbf{U} \sim \mathbf{U}^{k+1}$ we obtain the formula

$$J(\mathbf{U}^k)(\mathbf{U}^{k+1} - \mathbf{U}^k) = -\mathbf{F}(\mathbf{U}^k). \tag{7.36}$$

The new value $\mathbf{U}^{k+1}$ is sometimes relaxated with the parameter $\omega \in (0, 1)$

$$\mathbf{U}^{k+1} = \mathbf{U}^k + \omega J^{-1}(\mathbf{U}^k)(-\mathbf{F}(\mathbf{U}^k)). \tag{7.37}$$

In our computations we use $\omega = 0.7$ (see Section 5.4).

Chapter 8

Conclusion

The incompressible viscous flow in flexible tube in 1D approximation was formulated by the set of equations (3.72)-(3.82) as well as the initial and boundary conditions. Characteristics of the reduced system (3.83)-(3.84) were analytically determined. The numeric solution was searched by four independent numerical methods. Three of them – Crank-Nicholson, Euler and fractional step methods give very plausible results. The fourth method – the so-called "simple method" from Patankar give the different results for the nonstationar case.

The self-excited oscillations as well as the collapse of tube were simulated. We observe that the form of the frictional coefficient λ_f, function Φ (constants K_P, K_E) and the smoothness parameter T in the tube law (3.74) have a big influence on the numerical results. On the contrary the influence of the viscous parameter γ is negligible.

As a further extension we plan to add the chemical reactions, which participate in the remodeling of vessel walls (the creation of atherosclerotic plaques) and the consequent changes of their visco-elastic properties (the change of material constants; the form of the function Φ, parameters T and γ).

Another open problem is the question of modeling of vascular mechanical substitutes (the so-called "stents") with their influence on the hemodynamics in the cardiovascular system. The above mentioned problems will be necessary to solve in 2 and 3 dimensions.

Bibliography

[1] S.Hayashi, T.Hayasse, H.Kawamura (1998) Numerical analysis for stability and self-excited oscillations in collapsible tube flow. Journal of Biomechanical Engineering, Vol.120, pages 468-475.

[2] A.H.Shapiro (1977) Steady flow in collapsible tubes. ASME Journal of biomechanical engineering, Vol. 99, pages 126 - 147.

[3] S.V.Patankar. Numerical heat transfer and fluid flow, Hemisphere, Washington DC-New York.

[4] B.Bo Šrámek, J. Valenta, F. Klimeš. Biomechanics of the cardiovascular system. Publishing House of the Czech Technical University Publishers in Prague, 1995.

[5] J.Valenta, S.Konvičková. Biomechanika srdečně cévního systému. Biomechanics of the cardiovascular system. Publishing House of the Czech Technical University Press in Prague, 1997. [The Czech version of the previous publication].

[6] V.Třeška and others. Aneurysma břišní aorty. Grada Publishing, spol.s r.o., 1999.

[7] Stuart Ira Fox. Human Physiology, fifth edition. The McGraw-Hill Companies, Inc., 1996.

[8] F.Staněk, D.Karetová. Angiologie pro praxi. Maxdorf, spol. s r.o., 2001.

[9] F.Maršík, Světlana Přerovská. Fyziologické vlastnosti krve a její transport v kardiovaskulárním systému člověka. Institute of Thermomechanics, Academy of Sciences of the Czech Republic, 2001.

[10] V.Havlík, I.Marešová. Hydraulika, příklady. Publishing House of the Czech Technical University Press in Prague, 1997.

[11] M.Brdička, L.Samek, B.Sopko. Mechanika kontinua. Nakladatelství Academia, 2000.

[12] C.F.Colebrook. Turbulent flows in pipes with particular reference to the transition region between the smooth and rough pipe lawas. J.Institute Civil Eng., 1939.

[13] S.Turek. Efficient solvers for incompressible flow problems. Institut für Angewandte Mathematik, Universität Heidelberg, 1998.

[14] R.Glowinski, J.Periaux. Numerical methods for nonlinear problems in fluid dynamics, Proc.Intern. Seminar on Scientific Supercomputer, Paris. North-Holland, Feb. 2-6, 1987.

[15] S.Müller-Urbaniak. Eine Analyse des Zwischenschritt-θ-Verfahrens zir Lösung der instationären Navier-Stokes Gleichungen, Ph.D. Thesis, University of Heidelberg, 1993.

[16] J.Málek, J.Nečas, M.Rokyta. Weak and measured-valued solutions to evolutionary PDE‘s. Chapman and Hall/CRC, Applied Mathematics and Mathematical Computation 13, 1996.

[17] R.Barett, M.Berry, T.F.Chan, J.Demmel, J.Donato, J.Dongarra, V.Eijkhout, R.Pozo, C.Romine, and H.Van der Vorst. Templates for the solution of linear systems; Building blocks for iterative methods. SIAM, Philadelphia, PA, second edition, 1994.

Remarks